

Robust Power Control for Heterogeneous Users in Shared Unlicensed Bands

Saeedeh Parsaeefard, *Member, IEEE*, Mihaela van der Schaar, *Fellow, IEEE*,
and Ahmad R. Sharafat, *Senior Member, IEEE*

Abstract—We develop a robust formalism for power control games in unlicensed bands between two groups of users competing for the spectrum: informed-users (leaders) who have advanced capabilities to extract side-information about other users and their strategies, and uninformed-users (followers) who can only observe the aggregate interference caused by others. Such nominal leader-follower games have been previously studied in the power control literature; however, these prior works fail to capture an important aspect of such interactions: the side-information and observations made by users may be uncertain, which has an important impact on users' strategies and network performance. Thus, in this paper we propose a new, robust game-theoretic formalism and solution which takes these uncertainties into account. Specifically, each group chooses its actions by solving its respective worst-case robust optimization problems. We show how various types of uncertainties affect the social utility of each group, and identify in which deployment scenarios the social utility of the robust game is higher than that of the nominal game. Importantly, we show that robust solutions in such games are more energy efficient. Finally, our theoretical formalism, analysis and solutions are complemented by simulations.

Index Terms—Robust game theory, resource allocation, Stackelberg games, worst-case robust optimization.

I. INTRODUCTION

A. Motivation

VARIOUS dynamic spectrum sharing paradigms for licensed and unlicensed bands have been proposed in the literature to increase efficiency [1], [2]. In this context, one efficient and cost effective approach is to provide advanced capabilities to a portion of users (called informed-users) in order to extract side-information pertaining to other users, while the rest of users (called uninformed-users) can only observe the aggregate interference caused by others [3]. In this way, significant cost savings can be achieved since the cost of retrofitting the users' equipment pertains only to the informed-users group. The capabilities of each informed-user

include listening to the feedback channels and pilot signals of other users to extract side-information such as direct and interference channel gains of all users. Also, informed-users may have *a priori* side-information about transmit power constraints of other users and their objectives.

It has been shown in [3]–[6] that Stackelberg games provide a suitable framework to analyze equilibria for heterogeneous users. In this setup for unlicensed bands, the informed-users' objectives are similar to those of uninformed-users, and both groups enjoy the same priority. Each informed-user determines its optimal constrained transmit power to maximize its utility (e.g., its throughput) by estimating other users' transmit power levels via utilizing its side-information. Similarly, each uninformed-user determines its optimal constrained transmit power to maximize its own utility (e.g., its throughput) by utilizing its observation (interference caused by other users to its receiver). However, in practice, channel fading and users' mobility cause uncertainty in each user's side-information or observations, resulting in deviations from their expected utilities and in very undesirable fluctuations in their performances. Hence, it is essential to consider uncertainty in the utilities, side information, and observations of users.

Robust solutions have been proposed in the past decades for a variety of optimization problems to mitigate such uncertainties. Specifically, each uncertain parameter is modeled by the sum of its nominal (estimated) value and an additive error (the uncertain part) [7]. The optimization problem with nominal values (the nominal optimization problem) is mapped to its robust counterpart, in which each uncertain parameter is a new optimization variable [8]. Generally, two basic approaches are applied for this mapping [7], [8]: the Bayesian approach, where the statistics of error is considered and the utility is statistically guaranteed; and the worst-case approach, where the error is assumed to be bounded to the uncertainty region, and the utility is guaranteed for any realization of error in this region. Both approaches have been applied to respective games in communications, economics, and mathematics [9]–[12].

Since the worst-case approach preserves each user's utility under any condition of error in the uncertainty region, it prevents undesirable fluctuations in the performance of all users [13], [14]. Hence, we choose the worst-case approach to tackle uncertainty in parameter values. In [7], it is shown that the shape of the uncertainty region depends on the statistics of noise and the resulting error in wireless channels. We follow the terminology of robust optimization theory and call the Stackelberg game with nominal values and its corresponding

Manuscript received May 31, 2013; revised September 21 and December 26, 2013; accepted February 1, 2014. The associate editor coordinating the review of this paper and approving it for publication was M. Bhatnagar.

S. Parsaeefard and A. R. Sharafat (corresponding author) are with the Department of Electrical and Computer Engineering, Tarbiat Modares University, P. O. Box 14115-194, Tehran, Iran.

M. van der Schaar is with the Department of Electrical Engineering, University of California at Los Angeles (UCLA), Los Angeles, California, USA (e-mail: sharafat@modares.ac.ir).

This work was supported in part by Tarbiat Modares University, Tehran, Iran; in part by the Iran Telecommunications Research Center, Tehran, Iran under Ph.D. Research Grant TMU 88-11-124; and in part by NSF Grant CCF 0830556.

Digital Object Identifier 10.1109/TWC.2014.042314.130981

equilibrium as the nominal Stackelberg game (NSG), and the nominal equilibrium (NSE), respectively. When uncertainty in parameter values are considered and robust optimization is applied, we refer to the game and its equilibrium as the robust Stackelberg game (RSG) and the robust Stackelberg equilibrium (RSE), respectively.

To implement RSGs for heterogenous users, we encounter a number of challenges: **1)** How to define RSEs when informed-users and uninformed-users have different uncertain parameters? **2)** How to quantify the performance gap between the RSG and the NSG? **3)** How to reduce the complexity of solving the informed-user's robust optimization problem? **4)** How to generalize the RSG for multi-user scenarios?

Our key contributions in meeting the above challenges are summarized below:

1) *Studying the impact of uncertainty on the RSE:* We study the impact of uncertainty on the RSE by considering the following two cases: In Case 1, the uninformed-users' observations are noisy while informed-users possess accurate side-information; and in Case 2, informed-users' side-information and uninformed-users' observations are both noisy.

2) *Comparing the performance of the RSG with that of the NSG:* The Stackelberg game's performance corresponds to specific users' strategies and their utilities at its equilibrium. We show that for Case 1, uncertainty in the uninformed-users' observations decreases their utilities and increases the informed-users' utilities. In contrast, for Case 2, uncertainty in the informed-users' side-information decreases their utilities and increases the uninformed-users' utilities. For both cases, we derive the conditions under which the social utility (the sum of all user's utilities in the Stackelberg game) at the RSE is higher than that at its corresponding NSE. These deployment scenarios are very interesting because they show that introducing robustness can also improve the efficiency of spectrum utilization.

3) *Efficiently obtaining users' strategies at the RSE:* Obtaining users' strategies at the RSE entail many calculations for solving worst-case bi-level optimization problems. Our alternative is to derive the relationship between users' strategies at the RSE and at the NSE; and obtain the latter via existing efficient algorithms.

4) *Considering the multiple informed-users multiple uninformed-users scenario:* We begin our analysis of RSEs for the one informed-user one uninformed-user scenario, and generalize it to the multiple informed-users multiple uninformed-users scenario.

B. Related Works

Existing research relevant to this paper is either focused on the application of Stackelberg games for optimal power control in dynamic spectrum sharing environments for heterogenous users or on the theory of worst-case robust optimization in Stackelberg games. In general, transmit power optimization problems can be formulated either as cooperative utility (e.g., throughput) maximization problems as in [15]–[18], or as strategic non-cooperative games as in [19], [20]. In the first approach, globally optimal power allocation is guaranteed at the expense of a high computational complexity. To reduce

the computational cost, near optimal solutions have been proposed that utilize concepts such as relaxation algorithms [18], successive convex approximation for low complexity (SCALE) [21], difference-of-two-concave-functions (D.C.) approximation [22], non-negative matrix theory [16]–[18], or the Lagrange dual function [15]. Such schemes are usually implemented in a centralized manner, which need considerable message passing between synchronized users and the central point.

The alternative approach is to employ non-cooperative strategic games where users myopically maximize their utilities subject to their constraints and/or regulatory interference restrictions [15], [23]. In this approach, the notion of Nash equilibrium (NE) and its existence, uniqueness, robustness, as well as distributed algorithms for reaching the NE are widely studied in the literature, e.g., in [13], [14], [19], [20], [24], where each user only needs to know the interference of other users on its receiver. Hence, message passing is considerably reduced compared to that of the cooperative approach. However, a major practical issue is that the NE may be inefficient in terms of the achieved throughput as compared to that at the global optimum. The well-known approach to bridge this gap is to apply pricing as in [25], [26]. Moreover, the notion of variational inequalities is applied in [27] to select an equilibrium via applying a specific criteria (equilibrium selection approach). In Table I, we compare non-cooperative and cooperative approaches for solving power allocation problems.

In [3]–[6], it is shown that when advanced capabilities are added to a portion of users (informed-users) to extract side-information pertaining to all users, the achieved total throughput at the equilibrium for all users can be considerably higher without additional message passing. Here, the Stackelberg game is utilized to analyze the equilibrium of such hierarchical / bi-level interactions between two groups of users. In this paper, we extend this strand of literature to model interactions between non-cooperative heterogeneous users when exact values of system parameters are not available to respective users.

The theory of worst-case robust optimization can be applied to introduce robustness to the Stackelberg game's equilibrium against uncertainty in parameter values [10], [11], [28]. The closest works to this paper are [10], [11]. In [10], a one-leader one-follower Stackelberg game is considered where the leader's side-information is uncertain. By minimizing the second-order sensitivity function of the leader's utility with respect to the uncertain parameters, the worst-case utility for the leader can be obtained. In [11], three new algorithms based on mixed-integer linear-programming are proposed when the leader's side-information about the follower's response is uncertain due to the follower's bounded rationality, when the follower has noisy observations of the leader's strategy, and when the follower's reward is uncertain, respectively. In this paper, we analyze the effect of uncertainty on the achieved utilities of both the informed-users and the uninformed-users in different scenarios, and systematically consider various issues involved in implementing robust Stackelberg games in wireless networks. We also extend our study to multiple informed-users multiple uninformed-users games in wireless

TABLE I
COOPERATIVE VS. NON-COOPERATIVE APPROACHES TO SOLVE POWER CONTROL PROBLEMS

References	Optimization Problem	Approach	Sum Utility / Computational Complexity
[15]	Cooperative	Lagrange Dual Function	Near Optimal / Low
[16]	Cooperative	Non-Negative Matrix Theory	Global optima / High
[17], [18]	Cooperative	Relaxation / Non-Negative Matrix Theory	Local Optima / Low
[21], [22]	Cooperative	Convex Approximation	Local Optima / Low
[13], [14], [19], [20], [24]	Non-Cooperative	Strategic Game Theory	Inefficient / Low
[25]–[27]	Non-Cooperative	Strategic Game Theory	Pareto Optimal / Low

networks. In the rest of this paper, in line with existing literature and for convenience, we use “leader” for an informed-user, and “follower” for an uninformed-user. Table II summarizes the key differences between this paper and the existing literature.

Stackelberg games have also been used to model spectrum sharing by primary and secondary users in licensed bands. For example, in [29]–[34], the spectrum owner authorizes secondary users (SUs) to utilize the licensed band subject to a payoff by each SU, which is set in such a way to maximize the spectrum owner’s profit subject to the available spectrum and the SU’s power level. Note that the system model in this paper is completely different from those of the aforementioned works, as we are concerned only with spectrum sharing in unlicensed bands. Specifically, the use of Stackelberg games to formalize interactions among heterogeneous users does not necessarily entail a prioritization of transceivers. Rather, the formalism in this paper takes into account the asymmetry of side-information in heterogeneous users as in [3]–[5].

The rest of this paper is organized as follows. In Section II, the network model and proposed game formulations are presented, followed by a reformulation of these games with uncertainties in Section III. In Section IV, the robust Stackelberg equilibria are discussed and characterized. In Section V, we present a number of illustrative examples, and demonstrate that introducing robustness in such multi-user communication games can lead to important energy savings. In Section VI, we extend our framework to the multiple-leaders multiple-followers scenarios, followed by simulation results for these scenarios in Section VII, and conclusions in Section VIII.

II. PROBLEM FORMULATION

A. Network Model

Consider a set of $\mathcal{K} = \{1, \dots, K\}$ orthogonal frequency bands (sub-channels), which are shared between a set of $\mathcal{N} = \{0, 1, \dots, N\}$ users. Each user consists of one transmitter and one receiver. The transmit power of user n over all sub-channels is its set of possible actions denoted by $\mathcal{A}_n = \{\mathbf{p}_n = (p_n^1, \dots, p_n^K) | p_n^k \in [p_{n,k}^{\min}, p_{n,k}^{\max}], \forall k \in \mathcal{K}\}$. The utility of user n is $v_n(\mathbf{p})$, where $\mathbf{p} = [\mathbf{p}_n, \mathbf{p}_{-n}]$, and $\mathbf{p}_{-n} \triangleq [\mathbf{p}_0, \dots, \mathbf{p}_{n-1}, \mathbf{p}_{n+1}, \dots, \mathbf{p}_N]$ is a vector of other users’ transmit power levels except user n .

For the utility function of each user, we consider the following four assumptions:

A1) The utility of user n is strictly concave and differentiable function of \mathbf{p}_n , and its gradient is bounded.

A2) The utility function of user n is $v_n(\mathbf{p}_n, \mathbf{f}_n(\mathbf{p}_{-n}, \mathbf{s}_n)) = \sum_{k=1}^K v_n^k(p_n^k, f_n^k(\mathbf{p}_{-n}, \mathbf{s}_n))$, where $\mathbf{f}_n(\mathbf{p}_{-n}, \mathbf{s}_n) = [f_n^1(\mathbf{p}_{-n}, \mathbf{s}_n), \dots, f_n^K(\mathbf{p}_{-n}, \mathbf{s}_n)]$ is the $1 \times K$ vector of the linear aggregate impacts of other users on user n , in which $f_n^k(\mathbf{p}_{-n}, \mathbf{s}_n) = \sum_{m \in \mathcal{N}, m \neq n} p_m^k h_{nm}^k + \sigma_n^k$, and $\mathbf{s}_n \triangleq [\mathbf{h}_{n1}, \dots, \mathbf{h}_{n(n-1)}, \mathbf{h}_{n(n+1)}, \dots, \mathbf{h}_{nN}, \boldsymbol{\sigma}_n]$ denotes system parameters for user n , \mathbf{h}_{nm} is the $1 \times K$ vector whose element h_{nm}^k represents the sub-channel gain between user m and user n in sub-channel k , and $\boldsymbol{\sigma}_n = [\sigma_n^1, \dots, \sigma_n^K]$, where σ_n^k denotes channel noise-power in sub-channel k of user n .

A3) The utility of user n is a decreasing and convex function of $f_n^k(\mathbf{p}_{-n}, \mathbf{s}_n)$.

A4) The second order mixed partial derivatives of utility functions, i.e., $\frac{\partial^2 v_n^k}{\partial p_n^k \partial f_n^k}$ and $\frac{\partial^2 v_n^k}{\partial f_n^k \partial p_n^k}$, exist and are continuous.

Note that Assumption **A1** is commonly assumed in wireless networks [35]. In multiuser communication, Assumptions **A2** and **A3** are well known when users share the same resources and have a negative impact on each other [36]. Assumption **A4** indicates that the second order mixed partial derivatives of the utility of each user exist. Hence, Assumptions **A1**–**A4** are justified in practical multiuser wireless networks. In the illustrative examples in Section V, the utility of each user is its throughput, defined as $v_n(\mathbf{p}_n, \mathbf{f}_n(\mathbf{p}_{-n}, \mathbf{s}_n)) = \sum_{k=1}^K \log(1 + \frac{h_{nn}^k p_n^k}{f_n^k(\mathbf{p}_{-n}, \mathbf{s}_n)})$, which satisfies the above assumptions.

The rate of change in the throughput of user n is $\frac{\partial v_n^k(p_n^k, f_n^k(\mathbf{p}_{-n}, \mathbf{s}_n))}{\partial p_n^k} = \frac{h_{nn}^k}{f_n^k + h_{nn}^k p_n^k}$. When the direct channel gain for user n is high, i.e., $h_{nn}^k \gg 1$, or when its measured interference is low, i.e., $f_n^k \ll 1$, the value of $\frac{\partial v_n^k(p_n^k, f_n^k(\mathbf{p}_{-n}, \mathbf{s}_n))}{\partial p_n^k}$ is high. This means that a small change in the user’s action causes a significant change in its utility. The column gradient vector of v_n for user n , denoted by $\mathbf{J}_{\mathbf{p}_n}^n \triangleq \nabla_{\mathbf{p}_n} v_n(\mathbf{p}_n, \mathbf{f}_n(\mathbf{p}_{-n}, \mathbf{s}_n))$ is called the direct rate of user n , where the k^{th} element of this vector is $J_{\mathbf{p}_n}^{nk} = \frac{\partial v_n^k(p_n^k, f_n^k(\mathbf{p}_{-n}, \mathbf{s}_n))}{\partial p_n^k}$. Let $\mathbf{C}_{nm} \triangleq \mathbf{H}_{nm} \mathbf{J}_{\mathbf{f}_n}^n$, where $\mathbf{J}_{\mathbf{f}_n}^n \triangleq \nabla_{\mathbf{f}_n} v_n(\mathbf{p}_n, \mathbf{f}_n(\mathbf{p}_{-n}, \mathbf{s}_n))$ and $\mathbf{H}_{nm} \triangleq \text{diag}\{(h_{nm}^k)_{k=1}^K\}$. Note that \mathbf{C}_{nm} is the rate of decrease in the utility of user n caused by a corresponding increase in the action of user m . Hence, \mathbf{C}_{nm} is the negative impact of user m on user n for $m \neq n$. When the utility of user n is its throughput, we have $C_{nm}^k = -\frac{h_{nm}^k h_{nn}^k p_n^k}{f_n^k (f_n^k + h_{nn}^k p_n^k)}$, where C_{nm}^k is the k^{th} element of \mathbf{C}_{nm} . A high h_{nm}^k leads to a high C_{nm}^k , i.e., a high impact of user m on user n . We will use \mathbf{C}_{nm} and $\mathbf{J}_{\mathbf{p}_n}^n$ to compare the social utility at the RSE with that at the NSE.

TABLE II
COMPARISON OF EXISTING WORKS IN THE POWER CONTROL PROBLEM FOR HOMOGENOUS AND HETEROGENOUS USERS

References	Users	Equilibrium Type	Game Type	Equilibrium Coverage and Main Contributions
[15], [19], [23]	Homogeneous	Nash Equilibrium	Nominal	Existence and Uniqueness
[13], [14], [20]	Homogeneous	Nash Equilibrium	Robust	Existence and Uniqueness
[25]–[27]	Homogeneous	Nash Equilibrium	Nominal	Existence, Uniqueness, and Optimality
[3]–[6]	Heterogeneous	Stackelberg Equilibrium	Nominal	Existence and Optimality, 2) and 3) in Section I.A.
This paper	Heterogeneous	Stackelberg Equilibrium	Robust	Existence and Optimality, 1), 2), 3), and 4) in Section I.A.

B. Game Formulation

The above setup can be utilized for different game-theoretic formulations of the power control problem in cellular and wireless ad hoc networks [36]. In this paper, we consider power control games for spectrum sharing in unlicensed bands between two type of users: users with capabilities to extract side-information (leaders) and users without such capabilities (followers). Interactions between these two types of users can be modeled by a Stackelberg game [3], [4], where the sets of leaders and followers are $\mathcal{N}_L = \{0, 1, \dots, N_L - 1\}$ and $\mathcal{N}_F = \{1, \dots, N_F\}$, respectively, where N_L is the number of leaders and N_F is the number of followers, and $\mathcal{N} = \mathcal{N}_L \cup \mathcal{N}_F$ is the set of all users. In this setup, side-information obtained by user n is denoted by \mathcal{I}_n , which is empty for each follower (i.e., $\mathcal{I}_n = \emptyset$ if $n \in \mathcal{N}_F$) or contains side-information on other users for leaders (i.e., $\mathcal{I}_n = \{(\mathcal{A}_m, v_m, \mathbf{H}_{mn}, \mathbf{H}_{mm}, \mathbf{H}_{nm})_{m \neq n, \forall m \in \mathcal{N}}\}$ if $n \in \mathcal{N}_L$, where $\mathbf{H}_{mn} \triangleq \text{diag}\{(h_{mn}^k)_{k=1}^K\}$ and $\mathbf{H}_{mm} \triangleq \text{diag}\{(h_{mm}^k)_{k=1}^K\}$).

When users are non-cooperative and play a strategic game, the optimization problem of user n for choosing its transmit power is $\max_{\mathbf{p}_n \in \mathcal{A}_n} v_n(\mathbf{p}_n, \mathbf{f}_n(\mathbf{p}_{-n}, \mathbf{s}_n))$, whose solution is the best response of user n , denoted by $\mathbf{p}_n^*(\mathbf{p}_{-n})$. The Nash equilibrium (NE) of such a game, denoted by $[\mathbf{p}_0^*, \dots, \mathbf{p}_N^*]$, satisfies $v_n(\mathbf{p}_n^*, \mathbf{f}_n(\mathbf{p}_{-n}^*, \mathbf{s}_n)) \geq v_n(\mathbf{p}_n, \mathbf{f}_n(\mathbf{p}_{-n}^*, \mathbf{s}_n))$ for all $\mathbf{p}_n \in \mathcal{A}_n$, where $\mathbf{p}_{-n}^* \triangleq [\mathbf{p}_0^*, \dots, \mathbf{p}_{n-1}^*, \mathbf{p}_{n+1}^*, \dots, \mathbf{p}_N^*]$ for all $n \in \mathcal{N}$. From Assumption A1 in Section II.A and since \mathcal{A}_n is a closed and bounded set, it can be shown that the NE of this game always exists [37], [38]. While many sufficient conditions for NE's uniqueness can be obtained [19], [23], [39], NE's uniqueness in this paper is based on [23], [39].

The equilibrium in a Stackelberg game prescribes the optimal strategy set for leaders when followers play at their NE, and is derived via backward induction. For instance, for the one-leader one-follower Stackelberg game, where user 0 is the leader and user 1 is the follower, the leader knows that when it transmits with \mathbf{p}_0 , the follower's transmit power (its best response) is $\mathbf{p}_1^*(\mathbf{p}_0)$. Hence, the leader takes this into account in choosing its strategy. The leader's strategy at the Stackelberg equilibrium is $\mathbf{p}_0^{\text{NSE}}$ when for any $\mathbf{p}_0 \in \mathcal{A}_0$, we have $v_0(\mathbf{p}_0^{\text{NSE}}, \mathbf{f}_0(\mathbf{p}_1^*(\mathbf{p}_0^{\text{NSE}}), \mathbf{s}_0)) \geq v_0(\mathbf{p}_0, \mathbf{f}_0(\mathbf{p}_1^*(\mathbf{p}_0), \mathbf{s}_0))$. The Stackelberg equilibrium for the leader is the solution of the following bi-level optimization problem

$$\begin{aligned} & \max_{\mathbf{p}_0 \in \mathcal{A}_0} v_0(\mathbf{p}_0, \mathbf{f}_0(\mathbf{p}_1, \mathbf{s}_0)), \\ \text{subject to: } & \max_{\mathbf{p}_1 \in \mathcal{A}_1} v_1(\mathbf{p}_1, \mathbf{f}_1(\mathbf{p}_0, \mathbf{s}_1)). \end{aligned} \quad (1)$$

For the multi-follower scenario, the above backward procedure

is applicable as well. Let $\mathbf{p}_{-0}^*(\mathbf{p}_0) \triangleq [\mathbf{p}_1^*, \dots, \mathbf{p}_{N_F}^*]$ be the followers' strategies at their NE when the leader's strategy is \mathbf{p}_0 . The strategy profile $(\mathbf{p}_0^{\text{NSE}}, \mathbf{p}_{-0}^{\text{NSE}}(\mathbf{p}_0^{\text{NSE}}))$ is the equilibrium of the Stackelberg game iff $v_0(\mathbf{p}_0^{\text{NSE}}, \mathbf{f}_0(\mathbf{p}_{-0}^{\text{NSE}}(\mathbf{p}_0^{\text{NSE}}), \mathbf{s}_0)) \geq v_0(\mathbf{p}_0, \mathbf{f}_0(\mathbf{p}_{-0}^*(\mathbf{p}_0), \mathbf{s}_0))$, for any $\mathbf{p}_0 \in \mathcal{A}_0$, where $\mathbf{p}_{-0}^{\text{NSE}}(\mathbf{p}_0) = [\mathbf{p}_1^{\text{NSE}}, \dots, \mathbf{p}_{N_F}^{\text{NSE}}]$. At the NSE, the utility of user n is ω_n^{NSE} and the social utility of the game is $\omega^{\text{NSE}} = \sum_{n \in \mathcal{N}} \omega_n^{\text{NSE}}$. When the followers' game has multiple NEs, it is very complicated [40], [41]. We restrict our study to the Stackelberg game with a unique NE in the followers' game. The conditions for NE's uniqueness are presented in Section VI.

III. UNCERTAIN PARAMETERS

A. Noisy Observations

The uncertain value of $\tilde{\mathbf{f}}_n(\mathbf{p}_{-n}, \mathbf{s}_n)$ is a noisy observation by user n of the impact of other users, modeled by the sum of its nominal value and an error [7], i.e., $\tilde{\mathbf{f}}_n(\mathbf{p}_{-n}, \mathbf{s}_n) = \mathbf{f}_n(\mathbf{p}_{-n}, \mathbf{s}_n) + \hat{\mathbf{f}}_n(\mathbf{p}_{-n}, \mathbf{s}_n)$, where $\hat{\mathbf{f}}_n(\mathbf{p}_{-n}, \mathbf{s}_n) = [\hat{f}_n^1(\mathbf{p}_{-n}, \mathbf{s}_n), \dots, \hat{f}_n^K(\mathbf{p}_{-n}, \mathbf{s}_n)]$, $\mathbf{f}_n(\mathbf{p}_{-n}, \mathbf{s}_n) = [f_n^1(\mathbf{p}_{-n}, \mathbf{s}_n), \dots, f_n^K(\mathbf{p}_{-n}, \mathbf{s}_n)]$, and $\hat{\mathbf{f}}_n(\mathbf{p}_{-n}, \mathbf{s}_n) = [\hat{f}_n^1(\mathbf{p}_{-n}, \mathbf{s}_n), \dots, \hat{f}_n^K(\mathbf{p}_{-n}, \mathbf{s}_n)]$ are the noisy observation, the nominal value, and the error in the observation of user n , respectively. In the worst-case robust optimization, noisy observations for all $n \in \mathcal{N}_F$ are assumed to be in a bounded uncertainty region [39], [42] defined by

$$\mathfrak{R}_n(\mathbf{p}_{-n}) = \{\tilde{\mathbf{f}}_n(\mathbf{p}_{-n}, \mathbf{s}_n) \mid \|\hat{\mathbf{f}}_n(\mathbf{p}_{-n}, \mathbf{s}_n)\|_2 \leq \varepsilon_n\}, \quad (2)$$

where ε_n is the bound on the error, and $\|\cdot\|_2$ is the Euclidean norm. Since the Euclidean norm has been commonly used in wireless networks for modeling the uncertainty region in which all observations fall with a given probability [7], [13], we also use it in this paper. Note that the uncertainty region $\mathfrak{R}_n(\mathbf{p}_{-n})$ is not a fixed set and is a function of other users' strategies [43].

The noisy observation is considered as a new optimization variable in the utility of each follower [39]. In this case, the new utility function of follower n is $u_n(\mathbf{p}_n, \tilde{\mathbf{f}}_n(\mathbf{p}_{-n}, \mathbf{s}_n))$, which satisfies

$$u_n(\mathbf{p}_n, \tilde{\mathbf{f}}_n(\mathbf{p}_{-n}, \mathbf{s}_n))|_{\varepsilon_n=0} = v_n(\mathbf{p}_n, \mathbf{f}_n(\mathbf{p}_{-n}, \mathbf{s}_n)), \quad (3)$$

and the optimization problem of follower n is changed to

$$\max_{\mathbf{p}_n \in \mathcal{A}_n} \min_{\tilde{\mathbf{f}}_n(\mathbf{p}_{-n}, \mathbf{s}_n) \in \mathfrak{R}_n(\mathbf{p}_{-n})} u_n(\mathbf{p}_n, \tilde{\mathbf{f}}_n(\mathbf{p}_{-n}, \mathbf{s}_n)). \quad (4)$$

The NE of this robust game (the RNE) by assuming $\mathcal{I}_n = \emptyset$ for all followers is $\tilde{\mathbf{p}}^* = (\tilde{\mathbf{p}}_0^*, \dots, \tilde{\mathbf{p}}_N^*)$ [39], [42] iff $\min_{\tilde{\mathbf{f}}_n(\mathbf{p}_{-n}, \mathbf{s}_n) \in \mathfrak{R}_n(\mathbf{p}_{-n}^*)} u_n(\mathbf{p}_n^*, \tilde{\mathbf{f}}_n(\mathbf{p}_{-n}^*, \mathbf{s}_n)) \geq$

$\min_{\tilde{\mathbf{f}}_n(\mathbf{p}_{-n}, \mathbf{s}_n) \in \mathfrak{R}_n(\mathbf{p}_{-n}^*)} u_n(\mathbf{p}_n, \tilde{\mathbf{f}}_n(\mathbf{p}_{-n}^*, \mathbf{s}_n))$ for all $\mathbf{p}_n \in \mathcal{A}_n$. From Assumption A1 in Section II.A, the RNE exists for all channel gains between users, all bounded and closed strategy sets, and all uncertainty regions in (2) [39], [42]. We introduce a sufficient condition for uniqueness of the nominal NE in Section VI, which as shown in [39], [43] is also a sufficient condition for uniqueness of the RNE. However, solving (4) requires more calculations than solving the follower's optimization problem in the nominal game. To solve (4), each follower can utilize the numerical methods proposed in [44], [45] or semidefinite programming (SDP) (Proposition 1 in [44]).

B. Uncertain Side-Information

Obtaining the exact value of $\mathbf{H}_{n_F n_L}$ by the leader for all $n_F \in \mathcal{N}_F$ and $n_L \in \mathcal{N}_L$ is very challenging. This is because there is no pilot signal from the follower's receiver. Hence, we consider uncertainty in $\mathbf{H}_{n_F n_L}$, and denote its uncertain value by $\tilde{\mathbf{H}}_{n_F n_L}$. In the worst-case approach, $\hat{\mathbf{H}}_{n_F n_L}$ is the sum of its nominal value $\mathbf{H}_{n_F n_L}$ and the error $\hat{\mathbf{H}}_{n_F n_L}$, when the error is bounded to $\delta_{n_F n_L}$. The uncertainty region is

$$\mathcal{R}_{\mathbf{H}_{n_F n_L}} = \{ \tilde{\mathbf{H}}_{n_F n_L} \mid \| \hat{\mathbf{H}}_{n_F n_L} - \tilde{\mathbf{H}}_{n_F n_L} - \mathbf{H}_{n_F n_L} \|_2 \leq \delta_{n_F n_L} \}, \quad (5)$$

where the value of $\delta_{n_F n_L}$ depends on the pdf of noise, as explained in Section 8.5.5. in [7].

IV. ROBUST STACKELBERG EQUILIBRIUM

We now discuss the following two cases for the one-leader one-follower Stackelberg game:

Case 1) Leader's side-information is accurate, and follower's observation is noisy.

Case 2) Leader's side-information is uncertain, and follower's observation is noisy.

A. Analysis of RSE for Case 1

At the RSE for Case 1 (RSE1), the follower's optimization problem is (4). Moreover, the leader's side-information set is $\mathcal{I}_0^{\text{RSE1}} = \{ \mathcal{A}_1, v_1, \mathbf{H}_{10}, \mathbf{H}_{11}, \mathbf{H}_{01}, \mathfrak{R}_1(\mathbf{p}_0) \}$, and its bi-level optimization problem is

$$\begin{aligned} & \max_{\mathbf{p}_0 \in \mathcal{A}_0} v_0(\mathbf{p}_0, \mathbf{f}_0(\mathbf{p}_1, \mathbf{s}_0)), \\ \text{subject to: } & \max_{\mathbf{p}_1 \in \mathcal{A}_1} \min_{\tilde{\mathbf{f}}_1(\mathbf{p}_0, \mathbf{s}_1) \in \mathfrak{R}_1(\mathbf{p}_0)} u_1(\mathbf{p}_1, \tilde{\mathbf{f}}_1(\mathbf{p}_0, \mathbf{s}_1)). \end{aligned} \quad (6)$$

The best response of (4) to the leader's action is denoted by $\tilde{\mathbf{p}}_1^*(\mathbf{p}_0)$, and the leader's transmit power at RSE1, denoted by $\mathbf{p}_0^{\text{RSE1}}$, satisfies $v_0(\mathbf{p}_0^{\text{RSE1}}, \mathbf{f}_0(\tilde{\mathbf{p}}_1^*(\mathbf{p}_0^{\text{RSE1}}), \mathbf{s}_0)) \geq v_0(\mathbf{p}_0, \mathbf{f}_0(\tilde{\mathbf{p}}_1^*(\mathbf{p}_0), \mathbf{s}_0))$ for any $\mathbf{p}_0 \in \mathcal{A}_0$. In what follows, for notational convenience, we omit the arguments of $\mathbf{f}_n(\mathbf{p}_{-n}, \mathbf{s}_n)$.

Remark 1. RSE1 exists since: **1)** (4) is concave with respect to $\mathbf{p}_1(\mathbf{p}_0)$ for any fixed action of the leader, and is a decreasing function of \mathbf{f}_1 , and **2)** the two sets \mathcal{A}_1 and $\mathfrak{R}_1(\mathbf{p}_0)$ are convex, bounded, and disjoint. Consequently, there always exists a solution to (4) [44], and the optimization problem (6) has a non-empty feasible set. Hence, RSE1 exists. From the following lemma, we obtain RSE1.

Lemma 1. The leader's bi-level optimization problem can be rewritten as

$$\begin{aligned} & \max_{\mathbf{p}_0 \in \mathcal{A}_0} v_0(\mathbf{p}_0, \mathbf{f}_0) \\ \text{subject to: } & \max_{\mathbf{p}_1 \in \mathcal{A}_1} v_1(\mathbf{p}_1, \tilde{\mathbf{f}}_1^*), \end{aligned} \quad (7)$$

where

$$\tilde{\mathbf{f}}_1^* = \mathbf{f}_1 - \varepsilon_1 \boldsymbol{\vartheta}_1, \quad (8)$$

and $\tilde{\mathbf{f}}_1^* = [\tilde{f}_1^{1*}, \dots, \tilde{f}_1^{K*}]$, $\boldsymbol{\vartheta}_1 = [\vartheta_1^1, \dots, \vartheta_1^K]$, and ϑ_1^k is

$$\vartheta_1^k = \frac{\frac{\partial u_1^k(\mathbf{p}_1, \tilde{\mathbf{f}}_1^*)}{\partial f_1^k}}{\sqrt{\sum_{k=1}^K \left(\frac{\partial u_1^k(\mathbf{p}_1, \tilde{\mathbf{f}}_1^*)}{\partial f_1^k} \right)^2}}. \quad (9)$$

Proof: See Appendix A. \blacksquare

By utilizing (7) instead of (6), the uncertainty region is removed from the leader's optimization problem, and the leader's strategy and the follower's strategy as well as their respective utilities at RSE1 can be obtained and compared to those at the NSE.

Proposition 1. For Case 1 in the RSG:

1) The leader's action is an increasing function and the follower's action is a decreasing function of ε_1 , and are respectively obtained by

$$\mathbf{p}_0^{\text{RSE1}} = \mathbf{p}_0^{\text{NSE}} + \varepsilon_1 \times ((\mathbf{J}_{\mathbf{p}_0 \mathbf{p}_0}^0)^{-1} \mathbf{J}_{\mathbf{f}_0 \mathbf{p}_0}^0 \mathbf{H}_{01} (\mathbf{J}_{\mathbf{p}_1 \mathbf{p}_1}^1)^{-1} \mathbf{J}_{\mathbf{f}_1 \mathbf{p}_1}^1 \boldsymbol{\vartheta}_1^T)^T, \quad (10)$$

$$\mathbf{p}_1^{\text{RSE1}} = \mathbf{p}_1^{\text{NSE}} - \varepsilon_1 \times ((\mathbf{J}_{\mathbf{p}_1 \mathbf{p}_1}^1)^{-1} \mathbf{J}_{\mathbf{f}_1 \mathbf{p}_1}^1 \boldsymbol{\vartheta}_1^T)^T, \quad (11)$$

where $\mathbf{J}_{\mathbf{p}_n \mathbf{p}_n}^n \triangleq \text{diag}\{(\frac{\partial^2 v_n(\mathbf{p}_n, \mathbf{f}_n)}{\partial p_n^k})_{k=1}^K\}$, and $\mathbf{J}_{\mathbf{p}_n \mathbf{p}_n}^n \triangleq \text{diag}\{(\frac{\partial^2 v_n(\mathbf{p}_n, \mathbf{f}_n)}{\partial^2 p_n^k})_{k=1}^K\}$.

2) For any noisy observation of the follower, we have $\omega_0^{\text{NSE}} \leq \omega_0^{\text{RSE1}}$, and $\omega_1^{\text{RSE1}} \leq \omega_1^{\text{NSE}}$, where ω_n^{RSE1} is the utility of user n at RSE1.

3) The social utility at RES1 is $\omega^{\text{RSE1}} = \sum_{n \in \mathcal{N}} \omega_n^{\text{RSE1}}$, and we have $\omega^{\text{RSE1}} > \omega^{\text{NSE}}$, when C1 : $|\mathbf{C}_{10}| < |\mathbf{J}_{\mathbf{p}_0}^0|$ and C2 : $|\mathbf{J}_{\mathbf{p}_1}^1| < |\mathbf{C}_{01}|$, where $|\mathbf{q}|$ is the vector of absolute values of the elements of \mathbf{q} .

Proof: See Appendix B. \blacksquare

From Proposition 1, the solution to (6) can be obtained with considerably less calculations via the NSE and the bound on the uncertainty region in (10) and (11). Moreover, the leader's utility at RSE1 is higher than that at the NSE, while the follower's utility at RSE1 is less than that at the NSE. Interestingly, the social utility at RSE1 is higher than that at the NSE when C1 and C2 hold.

B. Analysis of RSE for Case 2

At the RSE for Case 2 (RSE2), $\tilde{\mathcal{I}}_0^{\text{RSE2}} = \{ \mathcal{A}_1, v_1, \tilde{\mathbf{H}}_{10}, \mathbf{H}_{11}, \mathbf{H}_{01}, \mathfrak{R}_1(\mathbf{p}_0) \}$ is the leader's uncertain side-information set, in which $\tilde{\mathbf{H}}_{10}$ is the uncertain parameter in the uncertainty region (5). Using worst-case optimization, the leader's bi-level optimization problem is changed to

$$\begin{aligned} & \max_{\mathbf{p}_0 \in \mathcal{A}_0} \min_{\tilde{\mathbf{H}}_{10} \in \mathcal{R}_{\mathbf{H}_{10}}} v_0(\mathbf{p}_0, \mathbf{f}_0), \\ \text{subject to: } & \max_{\mathbf{p}_1 \in \mathcal{A}_1} \min_{\tilde{\mathbf{f}}_1 \in \mathcal{R}_1(\mathbf{p}_0)} u_1(\mathbf{p}_1, \tilde{\mathbf{f}}_1). \end{aligned} \quad (12)$$

In (12), the leader cannot accurately evaluate its impact on the follower. Since \mathbf{f}_1 is a linear function of \mathbf{H}_{10} , and the leader considers the worst-case in the uncertainty region to obtain the solution of the follower, we have the following statement.

Statement 1. For Case 2, the negative impact of the leader on the follower is a decreasing function of δ_{10} , where δ_{10} was defined in (5).

Remark 2. RSE2 always exists, because: **1)** $\mathcal{R}_{\mathbf{H}_{10}}$, $\mathcal{R}_1(\mathbf{p}_0)$, \mathcal{A}_0 , and \mathcal{A}_1 are compact and closed sets, and **2)** for any realization of $\tilde{\mathbf{H}}_{10} \in \mathcal{R}_{\mathbf{H}_{10}}$, the uncertainty region $\mathcal{R}_1(\mathbf{p}_0)$ is closed and convex. Hence, the follower has a feasible strategy; and similar to Remark 1, RSE2 always exists.

While the condition for existence of RSE2 can be derived easily, solving (12) is significantly more complex than (6). This is because (12) has two uncertain parameters $\tilde{\mathbf{H}}_{10}$ and $\tilde{\mathbf{f}}_1$, and RSE2 is a function of both ε_1 and δ_{10} , while RSE1 is a function of ε_1 . To compare RSE1 and RSE2, ε_1 should have the same fixed value for both of these two cases. Next, we study the relationship between RSE1 and RSE2.

Proposition 2. For Case 2 in the RSG when ε_1 is fixed:

1) The leader's strategy is a decreasing function of δ_{10} and the follower's strategy is an increasing function of δ_{10} .

2) The leader's utility at RSE2 is always less than its utility at RSE1, i.e., $\omega_0^{\text{RSE2}} \leq \omega_0^{\text{RSE1}}$, where ω_n^{RSE2} is the utility of user n at RSE2 when the value of ε_1 is the same for RSE1 and RSE2.

Proof: See Appendix C. ■

To solve (12), for any value of \mathbf{p}_0 , the leader calculates the follower's transmit power from (4) via numerical methods in [44], [45] or via SDP reformulation in [44]. The leader also calculates its minimum utility corresponding to \mathbf{p}_0 , subject to $\tilde{\mathbf{H}}_{10} \in \mathcal{R}_{\mathbf{H}_{10}}$. Now, the leader chooses the value of \mathbf{p}_0 that corresponds to the maximum utility (its throughput) amongst all minimum utility values obtained for all $\mathbf{p}_0 \in \mathcal{A}_0$. Next, we compare the leader's and the follower's utilities at RSE2 with those at the NSE.

Proposition 3. For Case 2 in the RSG, when $\varepsilon_1 = 0$:

1) For all values of uncertain side-information in $\mathcal{R}_{\mathbf{H}_{10}}$, we have $\omega_0^{\text{RSE2}} \leq \omega_0^{\text{NSE}}$, and $\omega_1^{\text{NSE}} \leq \omega_1^{\text{RSE2}}$.

2) The social utility at RSE2 is $\omega^{\text{RSE2}} = \sum_{n \in \mathcal{N}} \omega_n^{\text{RSE2}}$, and we have $\omega^{\text{RSE2}} \geq \omega^{\text{NSE}}$, C3 : $|\mathbf{J}_{\mathbf{p}_0}^0| < |\mathbf{C}_{10}|$ and C4 : $|\mathbf{J}_{\mathbf{p}_1}^1| > |\mathbf{C}_{01}|$.

Proof: See Appendix D. ■

From Proposition 3, the leader's utility at RSE2 is less than that at the NSE, while the follower's utility at RSE2 is higher than that at the NSE. In this case, when the follower's direct rate is greater than its negative impact on the leader (i.e., C3), and the leader's direct rate is less than its negative impact on the follower (i.e., C4), the social utility at RSE2 is higher than that at the NSE. An interesting interpretation arises when comparing C1 with C3 and C2 with C4. These comparisons indicate that C1-C2 are the dual of C3-C4. In Case 1, a higher social utility can be achieved when the increase in the leader's utility is more than the decrease in the follower's utility. In contrast, in Case 2, a higher social utility can be achieved when the increment in the follower's utility is more than the decrement in the leader's utility.

V. ILLUSTRATIVE EXAMPLES

We now validate the above for the case in which the utility of each user is its throughput and C1-C4 are simplified for the estimated channel gains. In this case, (8) is $f_1^{*k} = f_1^k +$

$$\varepsilon_1 \times \frac{\frac{p_1^k h_{11}^k}{f_1^{*k} (f_1^{*k} + p_1^k h_{11}^k)}}{\sqrt{\sum_{k=1}^K \left(\frac{p_1^k h_{11}^k}{f_1^{*k} (f_1^{*k} + p_1^k h_{11}^k)} \right)^2}}$$

for all $k \in \mathcal{K}$. For the power control game, C1 is $\frac{h_{00}^k}{f_0^k + h_{00}^k p_0^k} > \frac{h_{10}^k h_{11}^k p_1^k}{f_1^k \times (f_1^k + h_{11}^k p_1^k)}$, and C2 is $\frac{h_{01}^k h_{10}^k p_0^k}{f_0^k \times (f_0^k + h_{00}^k p_0^k)} > \frac{h_{11}^k}{f_1^k + h_{11}^k p_1^k}$ for all k . Next, we consider the following three scenarios based on signal-to-interference-plus-noise ratios (SINRs) of the leader and the follower.

Scenario 1. High SINR, i.e., $h_{00}^k p_0^k \gg h_{01}^k p_1^k + \sigma_0^k$ and $h_{11}^k p_1^k \gg h_{10}^k p_0^k + \sigma_1^k$, where both C1 and C2 are simplified to

$$h_{01}^k > h_{10}^k. \quad (13)$$

Scenario 2. Low SINR, i.e., $h_{00}^k p_0^k \ll h_{01}^k p_1^k + \sigma_0^k$ and $h_{11}^k p_1^k \ll h_{10}^k p_0^k + \sigma_1^k$, where C1 and C2 are

$$h_{00}^k > h_{10}^k \quad \text{and} \quad h_{01}^k > h_{11}^k. \quad (14)$$

Scenario 3. Moderate SINR, i.e., $h_{00}^k p_0^k \approx f_0^k$ and $h_{11}^k p_1^k \approx f_1^k$, when interferences of the leader and the follower on each other are close, i.e., $f_1^k \approx f_0^k$, and both C1 and C2 become

$$h_{00}^k h_{01}^k > h_{11}^k h_{10}^k, \quad \forall k \in \mathcal{K}. \quad (15)$$

Considering the simplifications in (13)-(15), one can also obtain the probability of each scenario from the distribution of channel gains. As an example, for (13), when channels are Rayleigh fading and channel gains are i.i.d. random variables, the pdf of channel gains is exponential, i.e., $\phi(h_{01}^k) = \lambda_1 \exp^{-\lambda_1 h_{01}^k}$ and $\phi(h_{10}^k) = \lambda_2 \exp^{-\lambda_2 h_{10}^k}$. The probability $h_{01}^k > h_{10}^k$ is

$$\begin{aligned} & \int_0^\infty \int_0^{h_{01}^k} \phi(h_{01}^k) \phi(h_{10}^k) dh_{01}^k dh_{10}^k = \\ & \int_0^\infty \phi(h_{01}^k) dh_{01}^k (1 - \exp^{-\lambda_2 h_{01}^k}) = \\ & 1 - \frac{\lambda_1}{\lambda_1 + \lambda_2} = \frac{\lambda_2}{\lambda_1 + \lambda_2}. \end{aligned}$$

We use (13)-(15) to predict how the social utility changes for any given channel condition for Case 1. In doing so, we simulate a power control game in which a four-ray Rayleigh channel in [3] is assumed, $K = 20$, $p_{n,k}^{\text{max}} = 10$ mW, $p_{n,k}^{\text{min}} = 0$ and $\sigma_n = -80$ dBm. At the NSE, both the leader and the follower transmit at their maximum power $p_{n,k}^{\text{max}}$. At RSE1, the leader's and the follower's transmit power levels are obtained from (10) and (11), respectively. For RSE2, the leader for any $\mathbf{p}_0 \in \mathcal{A}_0$ and $\tilde{\mathbf{H}}_{10} \in \mathcal{R}_{\mathbf{H}_{10}}$, calculates the follower's transmit power from (4); and chooses its transmit power corresponding to the minimum throughput for $\tilde{\mathbf{H}}_{10} \in \mathcal{R}_{\mathbf{H}_{10}}$ and the maximum throughput for $\mathbf{p}_0 \in \mathcal{A}_0$. Subsequently, the follower measures \mathbf{f}_1 and calculates its optimal transmit power from (4). To compare the leader's and the follower's utilities when (13)-(15) hold, we use $d_n^{\text{RSE1}} = \frac{\omega_n^{\text{RSE1}} - \omega_n^{\text{NSE}}}{\omega_n^{\text{NSE}}}$ and $d^{\text{RSE1}} = \frac{\omega^{\text{RSE1}} - \omega^{\text{NSE}}}{\omega^{\text{NSE}}}$. A higher d_n^{RSE1} indicates a higher increment in the utility of user n for Case 1. For Case 2, we have $d_n^{\text{RSE2}} = \frac{\omega_n^{\text{RSE2}} - \omega_n^{\text{NSE}}}{\omega_n^{\text{NSE}}}$ and $d^{\text{RSE2}} = \frac{\omega^{\text{RSE2}} - \omega^{\text{NSE}}}{\omega^{\text{NSE}}}$ for the utility of user n and for

the social utility, respectively. In the following simulations, the bounds on the uncertainty regions are $\varepsilon_1 = \frac{\|\hat{\mathbf{f}}_1 - \mathbf{f}_1\|_2}{\|\mathbf{f}_1\|_2}$ and $\delta_{10} = \frac{\|\hat{\mathbf{H}}_{10} - \mathbf{H}_{10}\|_2}{\|\mathbf{H}_{10}\|_2}$. In simulations of this section, for one realization of CSIs, the uncertainty region is expanded to demonstrate the impact of uncertainty on the systems's performance.

Table III shows the leader's utility is incremented and the follower's utility is decremented when ε_1 is incremented, as expected from Proposition 1. When (13)-(15) hold, the social utility is incremented, and when (13)-(15) do not hold, it is decremented. In Scenario 1, the increment in the social utility is not considerable when (13) holds. In Scenarios 2 and 3, when (14) and (15) hold, the leader's utility and the social utility are incremented considerably. Note that when (14) does not hold, d_0^{RSE1} is reduced to 38.6% from 224.8%, and d_1^{RSE1} is reduced to -2.13% from 100.71% for $\varepsilon = 100\%$. Hence, playing the robust game when (14) and (15) hold, significantly increments the leader's utility and the social utility. This is achieved without increasing transmit power, i.e., a substantially better efficiency in utilizing spectrum and energy.

For Case 2, the constraints C3 and C4 in Proposition 3 become

$$\text{Scenario 1:} \implies h_{10}^k > h_{01}^k, \quad (16)$$

$$\text{Scenario 2:} \implies h_{10}^k > h_{00}^k, \text{ and } h_{11}^k > h_{01}^k, \quad (17)$$

$$\text{Scenario 3:} \implies h_{11}^k h_{10}^k > h_{00}^k h_{01}^k, \quad \forall k. \quad (18)$$

The effects of incrementing δ_{10} on d_0^{RSE2} , d_1^{RSE2} , and d^{RSE2} are shown in Table IV. Here, the value of ε_1 is set to 0 so that RSE2 can be clearly compared with NSE for different value of δ_{10} without considering the impact of ε_1 . As expected from Proposition 2, the leader's utility in all cases is less than that at the NSE, while the follower's utility is incremented by incrementing δ_{10} . In Table IV, when (16)-(18) do not hold, the social utility is decremented, and when (16)-(18) hold, it is incremented by incrementing δ_{10} , and d_1^{RSE2} is decremented as compared to when (16)-(18) do not hold. The ratio of channel gains for the above simulations are summarized in Table V.

In Tables III and IV, we note that in all scenarios for RSG2 when (16)-(18) hold, the increments in the follower's utility and the social utility are insignificant as compared to the increments in the leader's utility and the social utility at RSE1 when (13)-(15) hold. For example, in Scenario 2 for $\varepsilon = 100\%$, the leader's utility and the social utility at RSE1 are up to 200% and 100% higher than those at the NSE, respectively, whereas the follower's utility and the social utility at RSE2 are up to 10% and 2% higher than those at the NSE, respectively, meaning that a robust scheme significantly improves efficiency.

A. Power Control with Bounded Transmit Power

When the sum of transmit power levels of any user in all sub-channels is upper bounded to P_n^{\max} , i.e.,

$$\sum_{k=1}^K p_n^k \leq P_n^{\max}, \quad (19)$$

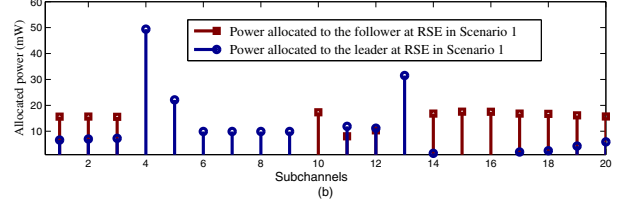
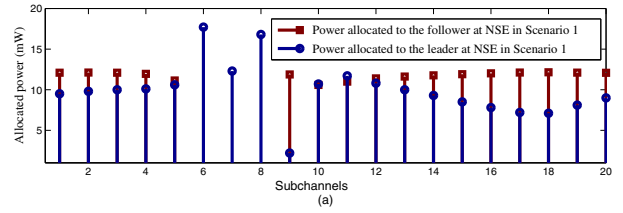


Fig. 1. Power allocation to the follower and to the leader in Scenario 1 subject to (19) - (a): at NSE, and (b): at RSE1.

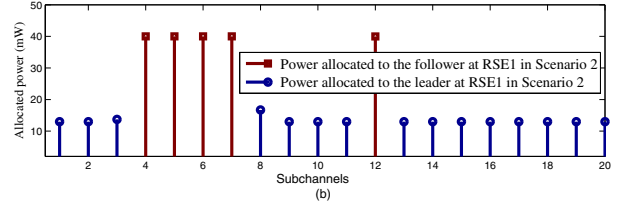
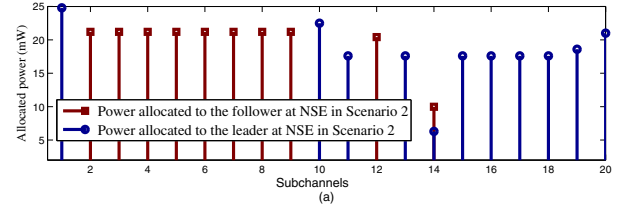


Fig. 2. Power allocation to the follower and to the leader in Scenario 2 subject to (19) - (a): at NSE, and (b): at RSE1.

the users' strategies are nonlinear functions of their observations [46]. Hence, we cannot use Propositions 1-3 to analyze the RSG. Transmit power levels in different sub-channels at RSE1 for (19) are shown in Figs. 1-3, and the corresponding changes in utility values are summarized in Table VI. Simulation parameters are the same as in Table III except for $P_n^{\max} = p_{n,k}^{\max} = 200$ mW, and $\varepsilon = 30\%$. For simulating the NSG by considering (19), we apply the algorithm in [3] to obtain transmit power levels. The follower's robust bi-level optimization problem at RSE1 is numerically solved for any transmit power of the leader.

To discuss the results of this case, let $\mathcal{K}_n^{\text{NSE}} \subseteq \mathcal{K}$ and $\mathcal{K}_n^{\text{RSE1}} \subseteq \mathcal{K}$ be the sets of sub-channels utilized by user n at the NSE and at RSE1, respectively. Also, let $\mathcal{L}_{nm}^{\text{NSE}} = \mathcal{K}_n^{\text{NSE}} \cap \mathcal{K}_m^{\text{NSE}}$ and $\mathcal{L}_{nm}^{\text{RSE1}} = \mathcal{K}_n^{\text{RSE1}} \cap \mathcal{K}_m^{\text{RSE1}}$ be the sets of sub-channels shared between user m and user n at the NSE and RSE1, respectively. Figs. 1-3 show that $|\mathcal{L}_{01}^{\text{RSE1}}| \leq |\mathcal{L}_{01}^{\text{NSE}}|$, where $|\mathcal{L}_{01}^{\text{RSE1}}|$ and $|\mathcal{L}_{01}^{\text{NSE}}|$ are the sizes of $\mathcal{L}_{01}^{\text{RSE1}}$ and $\mathcal{L}_{01}^{\text{NSE}}$, respectively. For example, in Scenario 1, we have $|\mathcal{L}_{01}^{\text{RSE1}}| = 10$ and $|\mathcal{L}_{01}^{\text{NSE}}| = 17$, and in Scenario 2, we have $|\mathcal{L}_{01}^{\text{RSE1}}| = 0$ and $|\mathcal{L}_{01}^{\text{NSE}}| = 1$. Table VI also shows that the leader's utility is incremented in Case 1 under all conditions.

Interestingly, in Scenario 2, the follower's utility at RSE1

TABLE III
VALIDATING PROPOSITION 1 VIA A NUMERICAL EXAMPLE FOR THE POWER CONTROL GAME

Scenario 1		$\varepsilon = 0$	$\varepsilon = 20\%$	$\varepsilon = 40\%$	$\varepsilon = 60\%$	$\varepsilon = 80\%$	$\varepsilon = 100\%$
(13) holds	d_0^{RSE1}	0	1.57	3.21	4.92	6.7	8.56
	d_1^{RSE1}	0	-1.7	-3.5	-5.33	-7.3	-9.2
	d_2^{RSE1}	0	0.02	0.03	0.037	0.045	0.045
(13) does not hold	d_0^{RSE1}	0	2.3	4.8	7.4	10.2	13.2
	d_1^{RSE1}	0	-2.14	-4.38	-6.75	-9.24	-11.9
	d_2^{RSE1}	0	-0.11	-0.21	-0.31	-0.4	-0.47
Scenario 2		$\varepsilon = 0$	$\varepsilon = 20\%$	$\varepsilon = 40\%$	$\varepsilon = 60\%$	$\varepsilon = 80\%$	$\varepsilon = 100\%$
(14) holds	d_0^{RSE1}	0	33.5	138.7	224.81	224.81	224.81
	d_1^{RSE1}	0	-35.6	-87.8	-100	-100	-100
	d_2^{RSE1}	0	7.1	52.15	100.71	100.71	100.71
(14) does not hold	d_0^{RSE1}	0	5.7	12.2	19.7	28.38	38.6
	d_1^{RSE1}	0	-4.27	-8.85	-13.82	-19.22	-25.13
	d_2^{RSE1}	0	-0.66	-1.24	-1.72	-2.04	-2.13
Scenario 3		$\varepsilon = 0$	$\varepsilon = 20\%$	$\varepsilon = 40\%$	$\varepsilon = 60\%$	$\varepsilon = 80\%$	$\varepsilon = 100\%$
(15) holds	d_0^{RSE1}	0	101.1	101.26	101.26	101.26	101.26
	d_1^{RSE1}	0	-100	-100	-100	-100	-100
	d_2^{RSE1}	0	53.7	53.8	53.8	53.8	53.8
(15) does not hold	d_0^{RSE1}	0	0.07	0.14	0.20	0.25	0.28
	d_1^{RSE1}	0	-0.06	-0.12	-0.17	-0.22	-0.26
	d_2^{RSE1}	0	-0.04	-0.07	-0.1	-0.13	-0.16

TABLE IV
VALIDATING PROPOSITION 2 VIA A NUMERICAL EXAMPLE FOR THE POWER CONTROL GAME

Scenario 1		$\delta_{10} = 0$	$\delta_{10} = 20\%$	$\delta_{10} = 40\%$	$\delta_{10} = 60\%$	$\delta_{10} = 80\%$	$\delta_{10} = 100\%$
(16) holds	d_0^{RSE2}	0	-0.23	-0.45	-0.67	-0.89	-1.12
	d_1^{RSE2}	0	0.18	0.37	0.55	0.74	0.92
	d_2^{RSE2}	0	0.002	0.004	0.005	0.007	0.008
(16) does not hold	d_0^{RSE2}	0	-0.31	-0.62	-0.92	-1.23	-1.53
	d_1^{RSE2}	0	0.31	0.62	0.93	1.23	1.53
	d_2^{RSE2}	0	-0.01	-0.02	-0.03	-0.04	-0.05
Scenario 2		$\delta_{10} = 0$	$\delta_{10} = 20\%$	$\delta_{10} = 40\%$	$\delta_{10} = 60\%$	$\delta_{10} = 80\%$	$\delta_{10} = 100\%$
(17) holds	d_0^{RSE2}	0	-3.86	-7.43	-10.72	-13.78	-16.63
	d_1^{RSE2}	0	2.94	5.74	8.4	10.99	13.46
	d_2^{RSE2}	0	0.49	0.99	1.51	2.05	2.59
(17) does not hold	d_0^{RSE2}	0	-6.65	-12.37	-17.4	-21.76	-25.7
	d_1^{RSE2}	0	8.7	16.7	24.24	31.24	37.8
	d_2^{RSE2}	0	-0.08	-1.25	-1.42	-1.47	-1.51
Scenario 3		$\delta_{10} = 0$	$\delta_{10} = 20\%$	$\delta_{10} = 40\%$	$\delta_{10} = 60\%$	$\delta_{10} = 80\%$	$\delta_{10} = 100\%$
(18) holds	d_0^{RSE2}	0	-1.47	-2.91	-4.3	-5.65	-6.96
	d_1^{RSE2}	0	0.65	1.29	1.91	2.53	3.13
	d_2^{RSE2}	0	0.24	0.47	0.69	0.93	1.157
(18) does not hold	d_0^{RSE2}	0	-5.86	-10.86	-15.2	-19.06	-22.49
	d_1^{RSE2}	0	11.99	23.01	33.2	42.7	51.5
	d_2^{RSE2}	0	-1.65	-2.88	-3.81	-4.51	-5.05

TABLE V
RATIO OF CHANNEL GAINS FOR TABLES III AND IV

	h_{10}^k/h_{00}^k	h_{01}^k/h_{11}^k
Scenario 1: (13) holds and (16) does not hold	< 0.1	> 0.2
Scenario 1: (13) does not hold and (16) holds	> 0.2	< 0.1
Scenario 2: (14) holds and (17) does not hold	< 1	> 1
Scenario 2: (14) does not hold and (17) holds	> 1	< 1
Scenario 3: (15) holds and (18) does not hold	< 0.1	> 0.9
Scenario 3: (15) does not hold and (18) holds	> 0.9	< 0.1

TABLE VI
CHANGES IN UTILITY VALUES SUBJECT TO (19)

	Scenario 1	Scenario 2	Scenario 3
Leader	28.1%	4.2%	30.1%
Follower	-24.5%	1.8%	-48%

is higher than that at the NSE. This is because when the number of shared sub-channels between the leader and the follower is reduced, there is less interference from the leader to the follower and vice versa at RSE1 as compared to the NSE. This means that as shown in Table VI, it is possible that both the leader's utility and the follower's utility are

increased simultaneously, resulting in improved spectrum and energy efficiency in the network. To study this increment in the follower's utility at RSE1, in Fig. 4, we depict the cumulative distribution function (CDF) of d_1^{RSE1} for the following examples.

Example 1: The leader's interference on the follower is high, e.g., $\frac{h_{10}^k}{h_{11}^k} > 0.8$, and the follower's interference on the leader is low, e.g., $\frac{h_{01}^k}{h_{00}^k} < 0.1$.

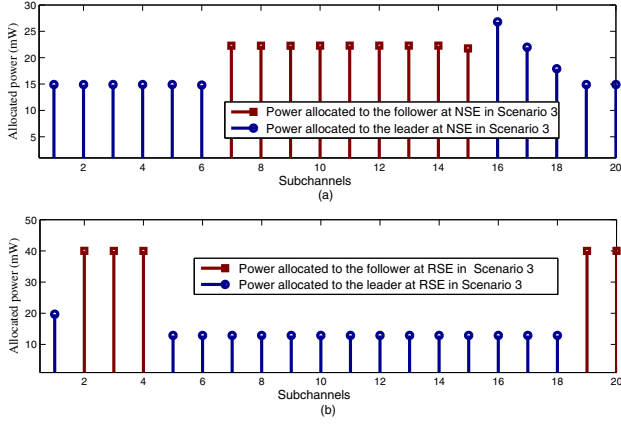


Fig. 3. Power allocation to the follower and to the leader in Scenario 3 subject to (19) - (a): at NSE, and (b): at RSE1.

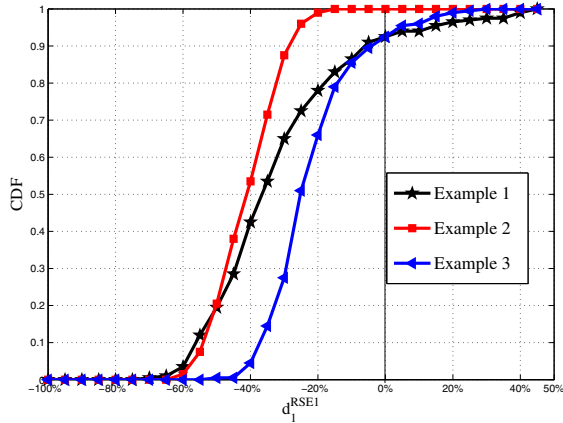


Fig. 4. CDF of d_1^{RSE1} when (19) holds

Example 2: The leader's and the follower's interference on each other are high, e.g., $\frac{h_{10}^k}{h_{11}^k} > 0.9$ and $\frac{h_{01}^k}{h_{00}^k} > 0.9$.

Example 3: The follower's interference on the leader is high, e.g., $\frac{h_{10}^k}{h_{11}^k} > 0.9$, and the leader's interference on the follower is low, e.g., $\frac{h_{01}^k}{h_{00}^k} < 0.1$.

Fig. 4 shows that in Example 2, the follower's utility at RSE1 is always below that at the NSE, whereas in Examples 1 and 3, with a probability of 10%, the follower's utility at RSE1 may be higher than that at the NSE. In such instances, the leader and the follower may achieve higher utilities when robustness is introduced to deal with uncertainty in the follower's observations, and transmit power is constrained as in (19), which results in a more efficient use of power and spectrum in wireless networks. Finally, in Table VII, for 10,000 channel realizations, we show the averaged impact of noise floor σ_n on the the number of shared sub-channels for both the RSG and the NSG. When noise floor is increased, the value of Lagrange multiplier associated with (19) is increased, which reduces the number of shared sub-channels between the leader and the follower for both the RSG and the NSG. Note that the number of shared sub-channels for the RSG is always below that for the NSG.

B. Energy Efficiency of RSG

Next, we compare power consumption in the NSG for increasing the leader's throughput as compared to that in the RSG for Case 1. In the NSG, when uncertainty is negligible and the leader wants to increase its throughput up to 100% in each sub-channel k for $p_0^k \in [p_{0,k}^{\min}, p_{0,k}^{\max}]$ for all $k \in \mathcal{K}$, the leader should increase $p_{0,k}^{\max}$ to $h_{00}^k (p_{0,k}^{\max})^2 / f_0^k$ to achieve its objective. However, as shown in Table III, the leader's throughput at RSE1 is incremented by 138.7% for Scenario 2 and $\varepsilon = 40\%$ without any increase in the leader's transmit power, meaning that the RSG for Case 1 is more energy efficient than the NSG.

Now consider a case in which (19) holds for both the leader and the follower, and the leader wants to increase its throughput. Simulation parameters are the same as in Section V.A. Let \hat{d}_0^{NSE} be the percentage of increase in the leader's throughput for different values of P_0^{\max} as compared to that for $P_0^{\max} = 200$ mW. In Table VIII, the values of \hat{d}_0^{NSE} are shown for $P_0^{\max} = 250$ mW and $P_0^{\max} = 300$ mW. In this table, $\hat{d}_0^{NSE} = 22.3\%$ for Scenario 1 at $P_0^{\max} = 300$ mW, while in Table VI, the value of \hat{d}_0^{RSE1} at $P_0^{\max} = 200$ mW is 28.1%. In other words, the increment in the leader's throughput is higher at RSE1 without increasing its transmit power as compared to that in the NSG with a significant increase in its transmit power.

In Scenario 2, increasing the leader's transmit power in the NSG increases its throughput more than that of considering uncertainties in the RSG. This is because in the NSG, when the follower's interference on the leader is high, increasing the leader's transmit power causes a proportional increase in its throughput; whereas at RSE1, when the follower's observation is uncertain, its interference on the leader is not decreased much. However, in Scenario 3, the increase in the leader's throughput for $P_0^{\max} = 300$ mW in the NSG is much less than that at RSE1; meaning that the same increase in the leader's throughput in the RSG can be achieved without increasing its transmit power, whereas in the NSG, it requires a significant increase in the leader's transmit power. The leader's throughput for $P_0^{\max} = 250$ mW at NSE for Scenarios 1 and 3 are much less than that at RSE1. In Scenarios 1 and 3, without increasing the leader's transmit power, its throughput is significantly higher at RSE1 as compared to that at NSE; meaning that in these scenarios, the RSG is energy efficient. In Table IV, the increments in the social utility and the utility of the follower at RSE2 are not considerable as compared to that at NSE, meaning that RSE2 is not as energy efficient as RSE1. For brevity, we do not discuss energy efficiency of RSE2 in this paper.

VI. EXTENSION TO MULTI-USER GAMES

A. One-Leader Multi-Follower ($N_L = 1$ and $N_F > 1$)

For this scenario, consider the $N_F \times N_F$ matrix Υ whose elements are

$$[\Upsilon]_{nm} = \begin{cases} \alpha_n^{\min} & \text{if } m = n, \quad m, n \in \mathcal{N}_F \\ -\beta_{nm}^{\max} & \text{if } m \neq n, \quad m, n \in \mathcal{N}_F, \end{cases}$$

where $\alpha_n(\mathbf{p}) \triangleq$ smallest eigenvalue of $-\nabla_{\mathbf{p}_n}^2 v_n(\mathbf{p}_n, \mathbf{f}_n)$, $\alpha_n^{\min} \triangleq \inf_{\mathbf{p} \in \mathcal{A}} \alpha_n(\mathbf{p})$, $\forall n \in \mathcal{N}_F$, $\beta_{nm}(\mathbf{p}) \triangleq$

TABLE VII
THE IMPACT OF NOISE FLOOR σ_n ON THE NUMBER OF SHARED SUB-CHANNELS FOR BOTH NSG AND RSG

	$\sigma_n = -80$ dBm	$\sigma_n = -60$ dBm	$\sigma_n = -40$ dBm
$\mathcal{L}_{nm}^{\text{NSE}}$	17.3	15.1	12.5
$\mathcal{L}_{nm}^{\text{RSE1}}$	15.9	12.7	11.1

TABLE VIII
 d_0^{NSE} SUBJECT TO (19) FOR DIFFERENT VALUES OF P_0^{max} IN NSG AS COMPARED TO THAT FOR $P_0^{\text{max}} = 200$ mW IN NSG

	Scenario 1		Scenario 2		Scenario 3	
P_0^{max} (mW)	250	300	250	300	250	300
d_0^{NSE}	12.6%	22.3%	13.3%	25%	13.9%	18.6%

$\|\nabla_{\mathbf{p}_n, \mathbf{p}_m} v_n(\mathbf{p}_n, \mathbf{f}_n)\|_2, \forall n \neq m, \beta_{nm}^{\text{max}} \triangleq \sup_{\mathbf{p} \in \mathcal{A}} \beta_n(\mathbf{p}), \forall n \in \mathcal{N}_F$.

When Υ is a P -matrix (Matrix Υ is a P -matrix if for any non-zero vector \mathbf{x} , we have $x_i(\Upsilon \mathbf{x})_i > 0$, where x_i is the i^{th} element of \mathbf{x} [38]), the followers' nominal NE and the RNE are unique (Theorem 12.5 in [47] and [39], [43]).

When the followers' game has multiple NEs, their distributed algorithm for reaching the equilibrium oscillates, and their equilibrium point depends on each follower's initial transmit power [27]. This leads to significant complications for the Stackelberg game [40], [41], and we do not consider it in this paper.

1) *RSE for Case 1 (RSE1)*: In this case, the followers' observations are uncertain, modeled by (2), but the leader has accurate side-information. The optimization problem of each follower is similar to (4), and reformulations to (8) and (9) can be applied [39] via

$$\tilde{\mathbf{f}}_n^* = \mathbf{f}_n - \varepsilon_n \vartheta_n, \quad \forall n \in \mathcal{N}_F, \quad (20)$$

where $\tilde{\mathbf{f}}_n^* = [\tilde{f}_n^{1*}, \dots, \tilde{f}_n^{K*}]$, $\vartheta_n = [\vartheta_n^1, \dots, \vartheta_n^K]$, and $\vartheta_n^k = \frac{\partial u_n^k(\mathbf{p}_n, \tilde{\mathbf{f}}_n^*)}{\partial f_n^k}$. Now, the algorithms proposed in [39] can be readily used to reach the RNE in a distributed manner for the above ϑ_n^k .

Remark 3. Since the RNE of the followers' game exists irrespective of parameters' values, and from Assumptions A1-A4 and \mathcal{A}_0 in Section II.A, the solution to the leader's optimization problem exists irrespective of interference caused by followers.

Proposition 4. For the above Case 1 of the RSG, when Υ is a P -matrix, we have:

1) The followers' strategies are decreasing functions of $\varepsilon = [\varepsilon_1, \dots, \varepsilon_N]$, and the social utility of the followers' game is less than that at the NSE.

2) The leader's utility at RSE1 is higher than that at the NSE.

3) The social utility at the RSE is higher than that at the NSE if C5 : $\mathbf{J}_{\mathbf{p}_0}^0 > \sum_{n \in \mathcal{N}_F} \mathbf{C}_{n0}$ and C6 : $\mathbf{J}_{\mathbf{p}_n}^n < \mathbf{C}_{0n} + \sum_{m \neq n, m \in \mathcal{N}_F} \mathbf{C}_{mn}$, for all $n \in \mathcal{N}_F$.

Proof: See Appendix E. ■

Similar to Proposition 1, noise in the followers' observations increments the leader's utility, but reduces the followers' utilities. When the leader's direct rate is higher than the sum of its negative impacts on all followers, i.e., C5, and when the sum of each follower's negative impacts on other followers

and on the leader is greater than its direct rate, i.e., C6, the social utility at RSE1 is higher than that at the NSE.

2) *RSE for Case 2 (RSE2)*: In this case, each follower's uncertainty is bounded to δ_{n0} , i.e.,

$$\mathcal{R}_{\mathbf{H}_{n0}} = \{\tilde{\mathbf{H}}_{n0} \mid \|\tilde{\mathbf{H}}_{n0}\|_2 = \|\tilde{\mathbf{H}}_{n0} - \mathbf{H}_{n0}\|_2 \leq \delta_{n0}\}. \quad (21)$$

Remark 4. Similar to RSE1, RSE2 always exists. Again, this is because the RNE for the followers' game always exists irrespective of the leader's side-information, and from Assumptions A1-A4 in Section II.A, Statement 1, and (21), the solution to the leader's optimization problem exists irrespective of the interference caused by followers.

Proposition 5. For Case 2, when $\varepsilon_n = 0$ and Υ is a P -matrix, we have:

1) The leader's utility at RSE2 is always less than that at the NSE.

2) The followers' actions are increasing functions of $\delta_0 = [\delta_{10}, \dots, \delta_{N_F0}]$, and the social utility of the followers' game at RSE2 is higher than that at the NSE.

3) The social utility is increased if C7 : $\mathbf{J}_{\mathbf{p}_0}^0 < \sum_{n \in \mathcal{N}_F} \mathbf{C}_{n0}$, and C8 : $\mathbf{J}_{\mathbf{p}_n}^n > \mathbf{C}_{0n} + \sum_{m \neq n, m \in \mathcal{N}_F} \mathbf{C}_{mn}$, for all $n \in \mathcal{N}_F$.

Proof: See Appendix F. ■

Again, uncertainty in the leader's side-information reduces its utility and increases the social utility of the followers. Also from C7-C8, when the leader's direct rate is less than the sum of its negative impacts on followers, and the sum of negative impacts of each follower on other followers and on the leader is less than its direct rate, the social utility at RSE2 is higher than that at the NSE. Besides, C5-C6 and C7-C8 are dual. For the one-leader multi-follower scenario, the leader derives its optimal solution using exhaustive search. In doing so, the step size is $\Theta_0^k = (p_{0,k}^{\text{max}} - p_{0,k}^{\text{min}})/\theta_0^k$, where $\theta_0^k \gg 1$. For any value of $\mathbf{p}_0 = (p_0^1, \dots, p_0^K)$ derived for this step size, i.e., $p_0^k = p_{0,k}^{\text{min}} + \Theta_0^k \times l$ where $0 \leq l \leq \theta_0^k$, the leader calculates the robust equilibrium for the followers' game via the algorithm in [39]. Subsequently, the leader calculates its utility based on the followers' transmit power levels at their equilibrium. The optimal value of \mathbf{p}_0 corresponds to the highest value of the leader's utility. The leader transmits at its optimal power level, and subsequently the followers play their strategic non-cooperative robust game. The followers can use the proposed algorithm in [39] to derive their optimal robust strategies.

B. Multi-Leader Multi-Follower ($N_L > 1$ and $N_F > 1$)

Since cooperation between leaders has been shown to improve spectrum efficiency [3], we consider such cooperation

for maximizing their social utility. Consider the leaders' optimization problem in the nominal game stated by

$$\begin{aligned} & \max_{\mathbf{p}_n \in \mathcal{A}_n} \sum_{n \in \mathcal{N}_L} v_n(\mathbf{p}_n, \mathbf{f}_n), \\ & \text{subject to: } \max_{\mathbf{p}_m \in \mathcal{A}_m} v_m(\mathbf{p}_m, \mathbf{f}_m), \quad \forall m \in \mathcal{N}_F. \end{aligned} \quad (22)$$

Note that (22) is a bi-level and non-convex optimization problem whose constraint involves the followers game [15]–[18]. Hence, it belongs to the class of mathematical programs with equilibrium constraints (MPEC), and in general, it is impossible to analytically solve (22). Instead, in [3], [6], numerical algorithms for solving (22) are proposed. Our approach for solving (22) and its robust counterpart is to randomly choose a leader who is tasked with obtaining the optimal transmit power vectors of all the leaders via exhaustive search. Since this leader is chosen randomly, there is no need for additional message passing among all the leaders for choosing a leader. We assume that all the leaders cooperate and provide their side-information only to the chosen leader, who would use such side-information in its exhaustive search for optimal transmit power vectors of all the leaders. Next, all the leaders transmit at their optimal power levels, and subsequently, the followers play their strategic non-cooperative game to obtain their own transmit power vectors.

For the multi-leader multi-follower game RSG1, the optimization problem of each follower is similar to (4). In this case, when Υ is a P -matrix, introducing robustness reduces the followers' interference on the leaders, and increases the leaders' utilities due to the fact that the followers' strategies at RSE1 are decreasing functions of ε_n (see Lemma 2 in Appendix E). In other words, the leaders' social utility at RSE1 is higher than that at the NSE.

For the multi-leader multi-follower game RSG2, the leaders' optimization problem is

$$\begin{aligned} & \max_{\mathbf{p}_n \in \mathcal{A}_n} \min_{\tilde{\mathbf{H}}_{nm} \in \mathcal{R}_{\mathbf{H}_{nm}}} \sum_{n \in \mathcal{N}_L} v_n(\mathbf{p}_n, \mathbf{f}_n), \\ & \text{subject to: } \max_{\mathbf{p}_m \in \mathcal{A}_m} \min_{\tilde{\mathbf{f}}_m \in \mathcal{R}_m(\mathbf{p}_{-m})} u_m(\mathbf{p}_m, \tilde{\mathbf{f}}_m), \quad \forall m \in \mathcal{N}_F, \end{aligned} \quad (23)$$

which is non-convex and MPEC. Hence, analyzing RSE2 is non-trivial. In Section VII, we propose a heuristic algorithm that converts the multi-leader multi-follower game into a one-leader multi-follower game. In the one-leader multi-follower game, the leader obtains its own transmit power vector via exhaustive search, and starts transmitting. Subsequently the followers play their own non-cooperative strategic game to obtain their respective transmit power vectors. In this way, the social utility at RSE2 is increased to the extent possible.

The above formulation maximizes each user's data rate subject to its transmit power constraints, and is also applicable for minimizing each user's transmit power subject to its minimum required data rate.

VII. SIMULATION RESULTS

We now simulate two cases of multi-leader multi-follower RSG in the power allocation problem for different bounds on the uncertainty region. In these simulations, ε_n is normalized to the estimated value of \mathbf{f}_n , i.e., $\varepsilon_n = \frac{\|\tilde{\mathbf{f}}_n - \mathbf{f}_n\|_2}{\|\mathbf{f}_n\|_2}$, and uncertainty for all users is assumed to be the same, denoted by ε . We

also have $\delta = \delta_{n_F n_L} = \frac{\|\tilde{\mathbf{H}}_{n_F n_L} - \mathbf{H}_{n_F n_L}\|_2}{\|\mathbf{H}_{n_F n_L}\|_2}$, $K = 20$, $\sigma_n^k = 0.01$ and the step size for exhaustive search $\Theta_n^k = (p_{n,k}^{\max} - p_{n,k}^{\min}) / \theta_n^k$ is set for $\theta_n^k = 100$ for all leaders and sub-channels.

A. One-Leader Multi-Follower ($N_L = 1$ and $N_F > 1$)

Let $N_F = 3$. All other parameters' values are the same as those of the illustrative examples in Section V and are equal for all users. To obtain the followers' actions, we utilize the numerical algorithm in [39]. To satisfy the NE's uniqueness condition, channel gains satisfy $h_{nm}^k < 0.01 h_{nn}^k$ for all $m, n \in \mathcal{N}_F$ and $m \neq n$. To hold C5 and C6, we assume that channel gains satisfy

$$\frac{h_{n0}^k}{h_{nn}^k} > 1 \quad \text{and} \quad \frac{h_{0n}^k}{h_{00}^k} < 1 \quad \forall k. \quad (24)$$

In this case, the followers' interference on each other is low, $C_{n0}^k \approx \frac{h_{nn}^k p_n^k}{p_0^k (h_{nn}^k p_n^k + h_{n0}^k p_0^k)}$, and $C_{n0}^k \ll 1$ because h_{n0} is high. Also, since the followers' interference on the leader is very low, we have $J_{p_0}^{0k} = \frac{h_{00}^k p_0^k}{h_{00}^k p_0^k + J_0^k} \approx 1$. Hence, C5 holds. The same argument can be made for C6. Consequently, when C5 and C6 do not hold, channel gains are such that (24) would not hold for all k .

Simulation results for this case are shown in Table IX, where $d_{-0}^{\text{RSE1}} = \frac{\omega_{-0}^{\text{RSE1}} - \omega_{-0}^{\text{NSE}}}{\omega_{-0}^{\text{NSE}}}$, $\omega_{-0}^{\text{RSE1}}$ is the social utility of the followers' game at RSE1, and ω_{-0}^{NSE} is the social utility of the followers' game at NSE. When ε is incremented, the leader's utility is increased, and d_{-0}^{RSE1} is reduced as expected from Proposition 4. Also, when C5 and C6 hold, the social utility of the robust Stackelberg game is increased, and is reduced when C5 and C6 do not hold. Note that when ε is incremented and C5 and C6 hold, the leader's utility is incremented more as compared to when ε is increased and C5 and C6 do not hold.

To simulate RSE2, we assume $\varepsilon_n = 0$, which means that the followers play the nominal game and $\delta = \delta_{n0}$ for all followers. For any value of $\tilde{\mathbf{H}}_{n0} \in \mathcal{R}_{\mathbf{H}_{n0}}$, the leader's RSE2 and the followers' NE are calculated; and for the minimum $\tilde{\mathbf{H}}_{n0}$, the leader's transmit power that maximizes its throughput is selected. The results are shown in Table X. To hold C7 and C8, channel gains should satisfy

$$\frac{h_{n0}^k}{h_{nn}^k} < 1 \quad \text{and} \quad \frac{h_{0n}^k}{h_{00}^k} > 1, \quad \forall k. \quad (25)$$

In Table X, we have $d_{-0}^{\text{RSE2}} = \frac{\omega_{-0}^{\text{RSE2}} - \omega_{-0}^{\text{NSE}}}{\omega_{-0}^{\text{NSE}}}$, where $\omega_{-0}^{\text{RSE2}}$ is the social utility of the followers' game at RSE2, and ω_{-0}^{NSE} is the social utility of the followers' game at NSE. Note that when C7 and C8 hold, the followers' social utility at RSE2 and the leader's utility are much higher than those at the NSE. This is because when the leader's interference channel gains are high, its interference is significantly decreased by reducing its strategy. Hence, the social utility is much higher at RSE2 than at NSE.

B. Multi-Leader Multi-Follower ($N_L > 1$ and $N_F > 1$)

Let $N_L = 2$, and $N_F = 8$. When interference between the two groups of users is low, the effect of changing transmit

TABLE IX
VALIDATING PROPOSITION 4 VIA A NUMERICAL EXAMPLE FOR THE POWER CONTROL GAME

		$\varepsilon = 20\%$	$\varepsilon = 40\%$	$\varepsilon = 60\%$			$\varepsilon = 20\%$	$\varepsilon = 40\%$	$\varepsilon = 60\%$
C5 and C6 hold	d_0^{RSE1}	1.45	1.99	2.46	C5 and C6 do not hold	d_0^{RSE1}	0.2	1.15	1.3
	d_{-0}^{RSE1}	-0.04	-0.3	-1.2		d_{-0}^{RSE1}	-0.05	-0.78	-2.33
	d^{RSE1}	1.2	1.3	1.41		d^{RSE1}	-0.13	-0.37	-1.33

TABLE X
VALIDATING PROPOSITION 5 VIA A NUMERICAL EXAMPLE FOR THE POWER CONTROL GAME

		$\delta = 20\%$	$\delta = 40\%$	$\delta = 60\%$			$\delta = 20\%$	$\delta = 40\%$	$\delta = 60\%$
C7 and C8 hold	d_0^{RSE2}	-0.61	-1.45	-2.67	C7 and C8 do not hold	d_0^{RSE2}	-0.14	-0.26	-0.45
	d_{-0}^{RSE2}	2.05	4.2	6.58		d_{-0}^{RSE2}	0.38	1.2	2
	d^{RSE2}	1.54	3.81	6.62		d^{RSE2}	-0.003	-0.006	-0.016

power via varying the uncertainty region is not visible in simulations. Hence, we assume that interference between the two groups is high. Simulation results for this case are summarized in Table XI, where a leader is randomly chosen to solve (22) via numerical search, and all other leaders pass their side-information to the selected leader. We have $\varepsilon = \varepsilon_n$ for all the followers, and $d_{\text{Leaders}}^{\text{RSE1}} = \frac{\omega_{\text{Leaders}}^{\text{RSE1}} - \omega_{\text{Leaders}}^{\text{NSE}}}{\omega_{\text{Leaders}}^{\text{NSE}}}$, where $\omega_{\text{Leaders}}^{\text{RSE1}}$ is the social utility of leaders from (22) at RSE1, and $\omega_{\text{Leaders}}^{\text{NSE}}$ is their social utility from (22) at the NSE. Other parameter values are the same as in Section VII.A.

In Table XI, $d_{\text{Leaders}}^{\text{RSE1}}$, d_{-0}^{RSE1} and d^{RSE1} are shown for 3 different cases: Case 1) interference between leaders are low, i.e., $\frac{h_{n_L n_L}}{h_{m_L n_L}} > 1$; Case 2) interference between leaders are moderate, i.e., $\frac{h_{n_L n_L}}{h_{m_L n_L}} \approx 1$; and Case 3) interference between leaders are high, i.e., $\frac{h_{n_L n_L}}{h_{m_L n_L}} < 1$, where in all cases, m_L and n_L belong to \mathcal{N}_L and $m_L \neq n_L$. Note that the leader's social utility is increasing with respect to ε , and the followers' social utility is decreasing with respect to ε , as expected from Section VI.B. The leaders' social utility in Cases 1 and 3 do not improve much as compared to those at the NSE, whereas in Case 2, the leaders' social utility is noticeably higher than that at the NSE. Note that variations in the leaders' social utility at RSE1 is not monotone, e.g., for Case 3, d^{RSE1} is decreasing with respect to ε for $\varepsilon < 60\%$, and is increasing at RSE1 for $60\% < \varepsilon < 80\%$. The reason being that in this case, the social utility is not convex, and its variations with respect to ε completely depend on channel gains.

As stated in Section VI.B, for the multi-leader multi-follower game RSG2, analysis of RSE2 is complicated. Nevertheless, as can be seen in Table X, when C7-C8 hold, at RSE2 of the one-leader multi-follower game, the social utility is significantly increased. In Table XII a heuristic algorithm for converting the multi-leader multi-follower RSG2 into a one-leader multi-follower RSG2 is presented. The number of leaders, denoted by N_L in Table XII, is *a priori* known, and leaders are arbitrarily indexed from 0 to $N_L - 1$. The algorithm scans the leaders until a candidate leader is found for whom C7-C8 hold. If no such leader is found, the candidate leader is the leader whose impact on all other players is the highest as compared to those of other leaders. The remaining leaders send their side-information to the candidate leader, who utilizes the same and obtains its own optimal transmit power vector via exhaustive search. Next, the candidate leader starts transmitting, and subsequently, the remaining leaders and the

followers are grouped together as the new set of followers, who would play their non-cooperative strategic game to obtain their respective transmit power vectors. Table XIII shows utility values obtained for $N_F = 1$ and $N_L = 2$. Parameter values are the same as in Table XI except for $\varepsilon = 0$ and $\delta = 30\%$.

To benchmark this algorithm, we consider 3 other options: 1) the NSG, 2) Leader 2 is chosen to lead RSG2 while Leader 1 acts as a follower (i.e., the game has two followers), and 3) at the global optima with no uncertainty. In Option 1, at NSE, the two leaders maximize the sum of their utilities via (22). When the leaders' side-information is uncertain, as per the heuristic algorithm in Table XII, the leader with highest interference on other leaders and followers (called Leader 1) acts as the leader and Leader 2 acts as the follower. This increases the social utility of the follower and Leader 2 at RSE2 and decreases the utility of Leader 1. In Option 2, Leader 2 acts as the leader, which causes its utility to be reduced, while the transmit power and utility of Leader 1 are increased. Since Leader 1's interference on other users is high, the utility of the follower and the social utility of game are considerably decreased. Table XIII shows that the utility at RSE2 for the heuristic algorithm has the closest social utility to that of the global optima among all options.

VIII. CONCLUSIONS

We modeled interactions among heterogeneous users competing for wireless spectrum as Stackelberg games, where leaders possess side-information about other users, while followers are reacting myopically solely based on their perceived interference levels. Different from past works, we explicitly considered uncertainty in the side-information and observations of users and its impact on their performances. To mitigate these uncertainties, we used the worst case robust approach, and analyzed two deployment scenarios: in the first one, leaders possess accurate side-information, while followers' observations are noisy; and in the second one, leaders possess inaccurate side-information and the followers' observations are noisy. We showed that the followers' noisy observations reduce their utilities and increase the leaders' utilities; while the leaders' inaccurate side-information reduces their utilities and increases the followers' utilities. We also derived the conditions under which an increase in social utilities can be achieved as a function of channel gains and experienced SINRs. Moreover, we provided insights on how to increase

TABLE XI
THE EFFECT OF UNCERTAINTY ON THE SOCIAL UTILITY OF THE MULTI-LEADER MULTI-FOLLOWER GAME

Case		$\varepsilon = 0$	$\varepsilon = 20\%$	$\varepsilon = 40\%$	$\varepsilon = 60\%$	$\varepsilon = 80\%$	$\varepsilon = 100\%$
Interference levels between leaders are high	$d_{\text{Leaders}}^{\text{RSE1}}$	0	0.14	0.26	0.45	1.9	2.1
	d_{-0}^{RSE1}	0	-6.22	-16.7	-25.8	-32.6	-38.4
	d^{RSE1}	0	-5.3	-9.4	-13.57	-20.22	-20.26
Interference levels between leaders are moderate	$d_{\text{Leaders}}^{\text{RSE1}}$	0	9.8	11.4	13.3	13.3	13.3
	d_{-0}^{RSE1}	0	-15.82	-18.71	-19.24	-19.24	-19.24
	d^{RSE1}	0	-5.97	-7.3	-5.97	-5.97	-5.97
Interference levels between leaders are low	$d_{\text{Leaders}}^{\text{RSE1}}$	0	0.1	0.15	0.2	0.64	1.3
	d_{-0}^{RSE1}	0	-5.2	-7.1	-9.4	-12.8	-13.64
	d^{RSE1}	0	-4.9	-6.3	-12.3	-9.6	-9.3

TABLE XII
HEURISTIC ALGORITHM FOR INCREASING SOCIAL UTILITY AT RSE2 FOR MULTI-LEADER MULTI-FOLLOWER GAME

Start $n_L = 0$.
 Consider $\mathcal{N}_F^{\text{new}} = \{0, \dots, n_L - 1, n_L + 1, \dots, N_L - 1\} \cup \mathcal{N}_F$
 Consider the leader indexed by n_L as the candidate leader and $\mathcal{N}_F^{\text{new}}$ as the new set of followers.
 Calculate C7-C8.
If C7-C8 hold for the candidate leader indexed by n_L :
 The candidate leader indexed by n_L obtains its optimal transmit power vector via exhaustive search.
 The candidate leader indexed by n_L starts transmitting.
 All the players in the set $\mathcal{N}_F^{\text{new}}$ are considered as followers, and play their non-cooperative strategic game.
Break.
Otherwise calculate $\mathbf{C}_{n_L} = \sum_{m \in \mathcal{N}_F^{\text{new}}} \mathbf{C}_{mn_L}$.
If $n_L = N_L - 1$:
 Find the candidate leader indexed by n_L such that $\mathbf{C}_{n_L} > \mathbf{C}_{m_L}, \forall m_L \in \mathcal{N}_L, m_L \neq n_L$.
 The candidate leader indexed by n_L obtains its optimal transmit power vector via exhaustive search.
 The candidate leader indexed by n_L starts transmitting.
 All the players in the set $\mathcal{N}_F^{\text{new}}$ are considered as followers, and play their non-cooperative strategic game.
Break.
Otherwise set $n_L = n_L + 1$.
Continue.

TABLE XIII
UTILITY VALUES OBTAINED VIA THE HEURISTIC ALGORITHM FOR THE MULTI-LEADER MULTI-FOLLOWER GAME

	Leader 1	Leader 2	Follower	All Followers	ω^{RSE2}
At NSE	5.06	4.33	2.08	6.41	11.47
At RSE2 for Heuristic Algorithm	4.97	4.19	2.49	6.68	11.65
At RSE2 when Leader 2 Leads RSG	5.01	4.09	1.97	6.06	11.07
At the Global Optima with No Uncertainty	4.23	5.12	3.35	8.47	12.7

the social utility in multi-leader multi-follower scenarios. An important direction for future research is to develop algorithms with less computations for multi-leader multi-follower scenarios in both nominal and robust games.

APPENDIX A PROOF OF LEMMA 1

From Assumption A3 in Section II.A, the inner optimization problem of the constraint in (6) is solved via the following Lagrange dual function [12]

$$L(\mathbf{a}_1, \tilde{\mathbf{f}}_1, \lambda_1) = \sum_{k=1}^K u_1^k(a_1^k, \tilde{f}_1^k) - \lambda_1 (\varepsilon_1^2 - \sum_{k=1}^K (\tilde{f}_1^k - f_1^k)^2), \quad (\text{A.1})$$

where λ_1 is the nonnegative Lagrange multiplier that satisfies

$$\lambda_1^* \times (\varepsilon_1^2 - \sum_{k=1}^K (\tilde{f}_1^{*k} - f_1^k)^2) = 0, \quad (\text{A.2})$$

where λ_1^* and \tilde{f}_1^{*k} are the optimal solutions to $L(\mathbf{a}_1, \tilde{\mathbf{f}}_1, \lambda_1)$. The solution to (A.1) for \tilde{f}_1^k is obtained from $\frac{\partial L(\mathbf{a}_1, \tilde{\mathbf{f}}_1, \lambda_1)}{\partial \tilde{f}_1^k} = 0$ [48], which is equivalent to $\frac{\partial u_1^k(a_1^k, \tilde{f}_1^k, \lambda_1)}{\partial \tilde{f}_1^k} = -2\lambda_1 \times (\tilde{f}_1^{*k} - f_1^k)$ for all $k \in \mathcal{K}$. Thus, the uncertain parameter is $\tilde{\mathbf{f}}_1^* = \mathbf{f}_1 - \varepsilon_1 \vartheta_1$, where $\tilde{\mathbf{f}}_1^* = [\tilde{f}_1^{*1}, \dots, \tilde{f}_1^{*K}]$, $\vartheta_1 = [\vartheta_1^1, \dots, \vartheta_1^K]$, and ϑ_1^k is (9).

APPENDIX B PROOF OF PROPOSITION 1

1) At RSE1, we have $\nabla_{\mathbf{p}_1^{\text{RSE1}}} u_1(\mathbf{p}_1^{\text{RSE1}}, \tilde{\mathbf{f}}_1^{\text{RSE1}}) \geq \mathbf{0}$, where $\mathbf{0}$ is the all zero $K \times 1$ vector, and

$$[\mathbf{J}_{\mathbf{p}_1 \mathbf{p}_1}^1 \nabla_{\varepsilon_1} \mathbf{p}_1^{\text{RSE1}} + \mathbf{J}_{\tilde{\mathbf{f}}_1 \mathbf{p}_1}^1 \nabla_{\varepsilon_1} \tilde{\mathbf{f}}_1^{\text{RSE1}}]_{\varepsilon_1=0} = \mathbf{0}. \quad (\text{B.1})$$

From (8), the last term on the left hand side of (B.1) is equal to $-\vartheta_1^T$. By rearranging (B.1), we have

$$\nabla_{\varepsilon_1} \mathbf{p}_1^{\text{RSE1}} = (\mathbf{J}_{\mathbf{p}_1 \mathbf{p}_1}^1)^{-1} \mathbf{J}_{\tilde{\mathbf{f}}_1 \mathbf{p}_1}^1 \vartheta_1^T. \quad (\text{B.2})$$

From Assumptions **A1-A3** in Section II.A, the right hand side of (B.2) is negative. Hence, $\nabla_{\varepsilon_1} \mathbf{p}_1^{*RSE1} < \mathbf{0}$, meaning that the follower's action is a decreasing function of ε_1 , and \mathbf{p}_1^{*RSE1} is obtained from (11).

At RSE1, we have $\nabla_{\mathbf{p}_0^{*RSE1}} v_0(\mathbf{p}_0^{*RSE1}, \mathbf{f}_0^{*RSE1}) \geq \mathbf{0}$, and

$$[\mathbf{J}_{\mathbf{p}_0 \mathbf{p}_0}^0 \nabla_{\varepsilon_1} \mathbf{p}_0^{*RSE1} + \mathbf{J}_{\mathbf{f}_0 \mathbf{p}_0}^0 \mathbf{H}_{01} \nabla_{\varepsilon_1} \mathbf{p}_1^{*RSE1}]_{\varepsilon_1=0} = \mathbf{0}, \quad (\text{B.3})$$

which is equivalent to

$$\nabla_{\varepsilon_1} \mathbf{p}_0^{*RSE1} = -(\mathbf{J}_{\mathbf{p}_0 \mathbf{p}_0}^0)^{-1} \mathbf{J}_{\mathbf{f}_0 \mathbf{p}_0}^0 \mathbf{H}_{01} \nabla_{\varepsilon_1} \mathbf{p}_1^{*RSE1}. \quad (\text{B.4})$$

From Assumptions **A1-A3** in Section II.A, the right hand side of (B.4) is positive. Hence, $\nabla_{\varepsilon_1} \mathbf{p}_0^{*RSE1} > \mathbf{0}$, meaning that the leaders' action is an increasing function of ε_1 , and \mathbf{p}_0^{*RSE1} is obtained from (10).

2) The Taylor series expansion of the leader's utility around the uncertain parameter is

$$v_0(\mathbf{p}_0^{*RSE1}, \mathbf{f}_0^{*RSE1}) = v_0(\mathbf{p}_0^{*NSE}, \mathbf{f}_0^{*NSE}) + \varepsilon_1 [(\mathbf{H}_{01} \mathbf{J}_{\mathbf{f}_0}^0)^T \nabla_{\varepsilon_1} \mathbf{p}_1^{*RSE1} + (\mathbf{J}_{\mathbf{p}_0}^0)^T \nabla_{\varepsilon_1} \mathbf{p}_0^{*RSE1}]_{\varepsilon_1=0} + o. \quad (\text{B.5})$$

In the sequel, we only consider the first term of the Taylor series¹ and ignore higher terms for small values of ε_1 . Based on Assumption **A2** in Section II.A and $\nabla_{\varepsilon_1} \mathbf{p}_1^{*RSE1} < \mathbf{0}$, the second term on the right hand side of (B.5) is always positive. Also, the third term on the right hand side of (B.5) has positive elements only. Hence, the leader's utility at RSE1 is always greater than that at the NSE, and we have

$$\omega_0^{*RSE1} - \omega_0^{*NSE} \approx \varepsilon_1 [(\mathbf{J}_{\mathbf{p}_0}^0)^T \nabla_{\varepsilon_1} \mathbf{p}_0^{*RSE1} + (\mathbf{H}_{01} \mathbf{J}_{\mathbf{f}_0}^0)^T \nabla_{\varepsilon_1} \mathbf{p}_1^{*RSE1}]. \quad (\text{B.6})$$

The Taylor series expansion of the follower's utility around ε_1 is

$$u_1(\mathbf{p}_1^{*RSE1}, \mathbf{f}_1^{*RSE1}) = v_1(\mathbf{p}_1^{*NSE}, \mathbf{f}_1^{*NSE}) + \varepsilon_1 [(\mathbf{H}_{10} \mathbf{J}_{\mathbf{f}_1}^1)^T \nabla_{\varepsilon_1} \mathbf{p}_0^{*RSE1} + (\mathbf{J}_{\mathbf{p}_1}^1)^T \nabla_{\varepsilon_1} \mathbf{p}_1^{*RSE1}]_{\varepsilon_1=0} + o. \quad (\text{B.7})$$

Since $\mathbf{J}_{\mathbf{f}_1}^1 < \mathbf{0}$ and $\nabla_{\varepsilon_1} \mathbf{p}_0^{*RSE1} > \mathbf{0}$, the second term on the right hand side of (B.7) is always negative. Also, $\nabla_{\mathbf{p}_1} v_1(\mathbf{p}_1, \mathbf{f}_1) > \mathbf{0}$ and $\nabla_{\varepsilon_1} \mathbf{p}_1^{*RSE1} < \mathbf{0}$. Consequently, the third term on the right hand side of (B.7) is negative. Hence, the follower's utility at RSE1 is always less than that at the NSE. After some rearrangements, we have

$$\omega_1^{*RSE1} - \omega_1^{*NSE} \approx \varepsilon_1 \times [(\mathbf{H}_{10} \mathbf{J}_{\mathbf{f}_1}^1)^T \nabla_{\varepsilon_1} \mathbf{p}_0^{*RSE1} + (\mathbf{J}_{\mathbf{p}_1}^1)^T \nabla_{\varepsilon_1} \mathbf{p}_1^{*RSE1}]. \quad (\text{B.8})$$

3) The social utility at RSE1 is increased when $\omega_0^{*RSE1} - \omega_0^{*NSE} + \omega_1^{*RSE1} - \omega_1^{*NSE} > 0$, which is equivalent to the sum of (B.6) and (B.8). To satisfy the above condition, note that since $\nabla_{\varepsilon_1} \mathbf{p}_1^{*RSE1} < \mathbf{0}$ and $\nabla_{\varepsilon_1} \mathbf{p}_0^{*RSE1} > \mathbf{0}$, the sum of the terms multiplied by $\nabla_{\varepsilon_1} \mathbf{p}_1^{*RSE1}$ should be negative and the sum of the terms multiplied by $\nabla_{\varepsilon_1} \mathbf{p}_0^{*RSE1}$ should be positive. Hence, we have $|\mathbf{J}_{\mathbf{p}_0}^0| - |\mathbf{H}_{10}| |\mathbf{J}_{\mathbf{f}_1}^1| > \mathbf{0}$, and $|\mathbf{J}_{\mathbf{p}_1}^1| - |\mathbf{H}_{01}| |\mathbf{J}_{\mathbf{f}_0}^0| < \mathbf{0}$, which are the same as C1 and C2.

¹In general, when higher order terms in the Taylor series are ignored, the comparison results hold in the neighborhood of the equilibrium at which Taylor series is applied. However, our approximation is for small values of ε_1 , meaning that the robust equilibrium which is a bounded perturbed version of the nominal equilibrium is in fact in its neighborhood, and higher order terms in the Taylor series can be ignored as they are multiplied by a higher power of ε_1 .

APPENDIX C

PROOF OF PROPOSITION 2

The proof of the first part of Proposition 2 is similar to the proof of the first part of Proposition 1, except that (B.2) is changed to

$$\nabla_{\delta_{10}} \mathbf{p}_1^{*RSE2} = \mathbf{M}_1 \nabla_{\delta_{10}} \mathbf{f}_1^{*RSE2}. \quad (\text{C.1})$$

From Statement 1 in Section IV.B, $\nabla_{\delta_{10}} \mathbf{p}_1^{*RSE2}$ is always positive, meaning that the follower's action is an increasing function of δ_{10} .

2) In this case, the leader cannot calculate the exact value of \mathbf{p}_1 from its incomplete side-information, meaning that the value of \mathbf{f}_0 is uncertain. Consequently, RSE2 can be considered as ϵ Stackelberg strategy space for Case 1 (Definition 4.7 in [49]) and hence, the leader's utility at RSE2 is less than that at RSE1.

APPENDIX D

PROOF OF PROPOSITION 3

1) The proof of this part is similar to the proof of the second part of Proposition 1 in Appendix B, except that (B.8) is changed to

$$\omega_1^{*RSE2} - \omega_1^{*NSE} \approx \delta_{10} \times [(\mathbf{J}_{\mathbf{p}_1}^1)^T (\mathbf{J}_{\mathbf{p}_1 \mathbf{p}_1}^1)^{-1} \mathbf{J}_{\mathbf{f}_1 \mathbf{p}_1}^1 \nabla_{\delta_{10}} \mathbf{f}_1^{*RSE2} - (\mathbf{J}_{\mathbf{f}_1}^1)^T \nabla_{\delta_{10}} \mathbf{f}_1^{*RSE2}]. \quad (\text{D.1})$$

From Assumptions **A1-A4** in Section II.A and Statement 1 in Section IV.B, the right hand side of (D.1) is positive. Hence, the follower's utility at RSE2 is higher than that at the NSE.

For the leader, we have similar steps as in Proposition 1, except that (B.6) is changed to

$$\omega_0^{*RSE2} - \omega_0^{*NSE} \approx \delta_{10} \times [-(\mathbf{J}_{\mathbf{p}_0}^0)^T (\mathbf{J}_{\mathbf{p}_0 \mathbf{p}_0}^0)^{-1} \mathbf{H}_{01} \mathbf{J}_{\mathbf{f}_0 \mathbf{p}_0}^0 + (\mathbf{J}_{\mathbf{f}_0}^0)^T \mathbf{H}_{01}] \nabla_{\delta_{10}} \mathbf{p}_1, \quad (\text{D.2})$$

which, from Assumptions **A1-A4** and Statement 1, is always negative. Hence, the leader's utility at RSE2 is less than that at the NSE.

2) Now we derive the conditions for increasing the social utility. Since $\nabla_{\delta_{10}} \mathbf{p}_0^{*RSE2} < \mathbf{0}$, the sum of the second term on the right hand side of (D.1), i.e., $(\mathbf{J}_{\mathbf{f}_1}^1)^T \nabla_{\delta_{10}} \mathbf{f}_1^{*RSE2} = (\mathbf{J}_{\mathbf{f}_1}^1)^T \mathbf{H}_{10} \nabla_{\delta_{10}} \mathbf{p}_1^{*RSE2}$, and the first term on the right hand side of (D.2), i.e., $-(\mathbf{J}_{\mathbf{p}_0}^0)^T (\mathbf{J}_{\mathbf{p}_0 \mathbf{p}_0}^0)^{-1} \mathbf{H}_{01} \mathbf{J}_{\mathbf{f}_0 \mathbf{p}_0}^0 = -(\mathbf{J}_{\mathbf{p}_0}^0)^T \nabla_{\delta_{10}} \mathbf{p}_0^{*RSE2}$, should be negative, i.e., $|\mathbf{J}_{\mathbf{p}_0}^0| - |\mathbf{J}_{\mathbf{f}_1}^1| |\mathbf{H}_{10}| < \mathbf{0}$. Also, since $\nabla_{\delta_{10}} \mathbf{p}_1^{*RSE2} > \mathbf{0}$, the sum of the first term on the right hand side of (D.1) and the second term on the right hand side of (D.2) should be positive, i.e., $|\mathbf{J}_{\mathbf{p}_1}^1| - |\mathbf{J}_{\mathbf{f}_0}^0| |\mathbf{H}_{01}| > \mathbf{0}$. Clearly, these two conditions are equivalent to C3 and C4.

APPENDIX E

PROOF OF PROPOSITION 4

Lemma 2. When Υ is a P -matrix, the followers' strategies are decreasing functions of $\varepsilon = [\varepsilon_1, \dots, \varepsilon_{N_F}]$.

Proof: Consider $\mathbf{p}_{N_F} \triangleq [\mathbf{p}_1, \dots, \mathbf{p}_{N_F}]$ and assume that \mathbf{p}_{N_F} is an increasing function of ε , i.e., $\mathbf{p}_{N_F}^{*RSE1} \geq \mathbf{p}_{N_F}^{*NSE}$. When Υ is a P -matrix, $\mathcal{J}(\mathbf{p}_{N_F}) \triangleq (\mathbf{J}_{\mathbf{p}_n}^n(\mathbf{p}))_{n=1}^{N_F}$ is strongly monotone (Theorem 12.5 in [47]), and

$$\mathcal{J}(\mathbf{p}_{N_F}^{*RSE1}) \geq \mathcal{J}(\mathbf{p}_{N_F}^{*NSE}). \quad (\text{E.1})$$

On the other hand, from (24), we have $\frac{\partial u_n^k(p_n^k, f_n^k)}{\partial p_n^k} = \frac{\partial v_n^k(p_n^k, \tilde{f}_n^{k*})}{\partial p_n^k} + \frac{\partial v_n^k(p_n^k, \tilde{f}_n^{k*})}{\partial f_n^{k*}} \times \frac{\partial \tilde{f}_n^{k*}}{\partial p_n^k}$, and

$$\frac{\partial \tilde{f}_n^{k*}}{\partial p_n^k} = \frac{\partial \tilde{f}_n^{k*}}{\partial v_n^k} \times \frac{\partial v_n^k}{\partial p_n^k} = -\varepsilon_n \times \frac{\partial^2 v_n^k(\mathbf{p}_n, \tilde{f}_n^*)}{\partial p_n^k \partial \tilde{f}_n^k} \times \left(\sum_{k=1}^K \left(\frac{\partial u_n^k(\mathbf{p}_n, \tilde{f}_n^*)}{\partial f_n^k} \right)^2 \right)^{-\frac{1}{2}}. \quad (\text{E.2})$$

Consider $\tilde{p}_n^k = -\varepsilon_n \times \frac{\partial v_n^k(\mathbf{p}_n, \tilde{f}_n^*)}{\partial f_n^{k*}} \times \frac{\partial^2 v_n^k(\mathbf{p}_n, \tilde{f}_n^*)}{\partial p_n^k \partial f_n^{k*}} \times \left(\sum_{k=1}^K \left(\frac{\partial u_n^k(\mathbf{p}_n, \tilde{f}_n^*)}{\partial f_n^{k*}} \right)^2 \right)^{-\frac{1}{2}} \Big|_{\mathbf{p}_n = \mathbf{p}_n^{\text{NSE}}}$, which is negative according to Assumptions **A1-A3** in Section II.A. We rewrite (E.2) as $\mathcal{J}(\mathbf{p}_{N_F}^{\text{RSE1}}) - \mathcal{J}(\mathbf{p}_{N_F}^{\text{NSE}}) = \tilde{\mathbf{p}} < \mathbf{0}$, where $\tilde{\mathbf{p}} = (\tilde{p}_n)_{n=1}^{N_F}$, $\tilde{\mathbf{p}}^T = [\tilde{p}_1, \dots, \tilde{p}_K]$, and $\mathbf{0}$ is the zero vector whose size is the same as $\tilde{\mathbf{p}}$. Obviously, this contradicts (E.1), and implies that our assumption was wrong. Consequently, the followers' actions at RSE1 are decreasing functions of ε . ■

1) Since the followers' strategies are decreasing functions of ε , \mathbf{f}_0 is reduced by increasing ε , which implies $\omega_0^{\text{RSE1}} \geq \omega_0^{\text{NSE}}$ from Assumption **A2** in Section II.A and the Taylor series expansion of v_0^{RSE1} around ε , which is

$$\omega_0^{\text{RSE1}} = \omega_0^{\text{NSE}} + \varepsilon_n \times [(\nabla_{\varepsilon} \mathbf{p}_0)^T \mathbf{J}_{\mathbf{p}_0}^n + \sum_{n=1}^{N_F} \mathbf{H}_{0n} \mathbf{J}_{\mathbf{f}_0}^n (\nabla_{\varepsilon} \mathbf{p}_n)^T] + o. \quad (\text{E.3})$$

2) The RNE of the followers in the multi-follower RSG in Section VI.A belongs to the robust additively coupled games introduced in [39]. From Theorem 2 in [39], when Υ is a P -matrix, the followers' social utility at RSE1 is less than that at the NSE. Also, the Taylor series expansion of the utility of follower n around ε is

$$\omega_n^{\text{RSE1}} = \omega_n^{\text{NSE}} + \varepsilon_n \times [(\mathbf{J}_{\mathbf{f}_n}^n)^T \mathbf{H}_{n0} \nabla_{\varepsilon} \mathbf{p}_0 + (\mathbf{J}_{\mathbf{f}_n}^n)^T \left(\sum_{m=1, m \neq n}^{N_F} \mathbf{H}_{nm} \nabla_{\varepsilon} \mathbf{p}_m \right) + (\mathbf{J}_{\mathbf{p}_n}^n)^T \nabla_{\varepsilon} \mathbf{p}_n] + o, \quad (\text{E.4})$$

where $\nabla_{\varepsilon} \mathbf{p}_0$ is the $K \times 1$ vector whose k^{th} element is $\sum_{n \in \mathcal{N}_F} \frac{\partial p_0^k}{\partial \varepsilon_n}$.

3) When the sum of (E.3) and (E.4) is positive, the social utility at RSE1 is higher than that at the NSE. To satisfy this condition, the terms multiplied by $\nabla_{\varepsilon} \mathbf{p}_0$ should be positive because $\nabla_{\varepsilon} \mathbf{p}_0 > \mathbf{0}$. Since $\nabla_{\varepsilon} \mathbf{p}_n < \mathbf{0}$, the terms multiplied by $\nabla_{\varepsilon} \mathbf{p}_n$ should be negative. By some rearrangements, positiveness of the terms multiplied by $\nabla_{\varepsilon} \mathbf{p}_0$ and negativeness of the terms multiplied by $\nabla_{\varepsilon} \mathbf{p}_n$ lead to C5 and C6.

APPENDIX F

PROOF OF PROPOSITION 5

The proof is similar to the proof of Proposition 4, except that instead of Lemma 2, here we have the following lemma.

Lemma 3. When Υ is a P -matrix, the followers' strategies are increasing functions of $\delta_0 \triangleq [\delta_{10}, \dots, \delta_{N_F0}]$.

Proof: The proof is similar to that of Lemma 2 in Appendix E, except that here, we assume that the followers' strategies are decreasing functions of δ_0 , and demonstrate that this assumption contradicts Assumptions **A1-A4** in Section II.A and Statement 1 in Section IV.B. ■

1) Now, (E.3) is changed to

$$\omega_0^{\text{RSE2}} = \omega_0^{\text{NSE}} + \delta_{n0} \times \left[\sum_{n \in \mathcal{N}_F} (\mathbf{J}_{\mathbf{f}_0}^n)^T \mathbf{H}_{0n} \nabla_{\delta_{n0}} \mathbf{p}_n + (\mathbf{J}_{\mathbf{p}_0}^0)^T \nabla_{\delta_{n0}} \mathbf{p}_0 \right] + o. \quad (\text{F.1})$$

2) Also, (E.4) is changed to

$$\omega_n^{\text{RSE2}} = \omega_n^{\text{NSE}} + \delta_{n0} \times [(\mathbf{J}_{\mathbf{f}_n}^n)^T \mathbf{H}_{n0} \nabla_{\delta_{n0}} \mathbf{p}_0 + (\mathbf{J}_{\mathbf{f}_n}^n)^T \left(\sum_{m \neq n, m \in \mathcal{N}_F} \mathbf{H}_{nm} \nabla_{\delta_{m0}} \mathbf{p}_m \right) + (\mathbf{J}_{\mathbf{p}_n}^n)^T \nabla_{\delta_{n0}} \mathbf{p}_n] + o. \quad (\text{F.2})$$

3) When the sum of the second terms in (F.1) and (F.2) for all followers are positive, the social utility at RSE2 is higher than that at the NSE. To satisfy this condition, since $\nabla_{\delta_{n0}} \mathbf{p}_0 < \mathbf{0}$ and $\nabla_{\delta_{n0}} \mathbf{p}_n > \mathbf{0}$, the terms multiplied by $\nabla_{\delta_{n0}} \mathbf{p}_0$ should be negative, and the terms multiplied by $\nabla_{\delta_{n0}} \mathbf{p}_n$ should be positive. By some rearrangements, C7 and C8 are obtained.

REFERENCES

- [1] J. Peha, "Sharing spectrum through spectrum policy reform and cognitive radio," *Proc. IEEE*, vol. 97, no. 4, pp. 708–719, Apr. 2009.
- [2] A. Goldsmith, S. A. Jafar, I. Maric, and S. Srinivasa, "Breaking spectrum gridlock with cognitive radios: an information theoretic perspective," *Proc. IEEE*, vol. 97, no. 5, pp. 894–914, May 2009.
- [3] Y. Su and M. van der Schaar, "A new perspective on multi-user power control games in interference channels," *IEEE Trans. Wireless Commun.*, vol. 8, no. 6, pp. 2910–2919, June 2009.
- [4] —, "Decentralized knowledge and learning in strategic multi-user communication," 2011. Available: <http://arxiv.org/abs/0804.2831>.
- [5] L. Lai and H. El Gamal, "The water-filling game in fading multiple-access channels," *IEEE Trans. Inf. Theory*, vol. 54, no. 5, pp. 2110–2122, May 2008.
- [6] S. Gurucharya, D. Niyato, D. I. Kim, and E. Hossain, "Hierarchical competition for downlink power allocation in OFDMA femtocell networks," *IEEE Trans. Wireless Commun.*, vol. 12, no. 4, pp. 1543–1553, Apr. 2013.
- [7] A. B. Gershman and N. D. Sidiropoulos, *Space-Time Processing for MIMO Communications*. John Wiley and Sons, 2005.
- [8] A. Ben-Tal and A. Nemirovski, "Selected topics in robust convex optimization," *Mathematical Programming*, vol. 112, no. 1, pp. 125–158, July 2007.
- [9] T.-S. Chang and Y.-C. Ho, "Stochastic Stackelberg games: non-nested multi-stage multi-agent incentive problems," *IEEE Trans. Autom. Control*, vol. 28, no. 4, pp. 477–488, Apr. 1983.
- [10] D. H. Cansever and T. Basar, "A minimum sensitivity approach to incentive design problems," *Large Scale Syst.*, vol. 5, pp. 233–244, 1983.
- [11] J. Pita, M. Jain, M. Tambe, F. Ordóñez, and S. Kraus, "Robust solutions to Stackelberg games: addressing bounded rationality and limited observations in human cognition," *Artificial Intelligence*, vol. 174, no. 15, pp. 1142–1171, Oct. 2010.
- [12] W. A. Brock and S. N. Durlauf, "Local robustness analysis: theory and application," *Elsevier J. Economic Dynamics Control*, vol. 29, no. 11, pp. 2067–2092, Nov. 2005.
- [13] P. Setoodeh and S. Haykin, "Robust transmit power control for cognitive radio," *Proc. IEEE*, vol. 97, no. 5, pp. 915–939, May 2009.
- [14] A. J. G. Anandkumar, A. Anandkumar, S. Lambotaran, and J. Chambers, "Robust rate maximization game under bounded channel uncertainty," *IEEE Trans. Veh. Technol.*, vol. 60, no. 9, pp. 4471–4486, Nov. 2011.
- [15] Z.-Q. Luo and S. Zhang, "Dynamic spectrum management: complexity and duality," *IEEE J. Sel. Topics Signal Process.*, vol. 2, no. 1, pp. 57–72, Feb. 2008.
- [16] C. W. Tan, S. Friedland, and S. H. Low, "Spectrum management in multiuser cognitive wireless networks: optimality and algorithm," *IEEE J. Sel. Areas Commun.*, vol. 29, no. 2, pp. 421–430, Dec. 2011.
- [17] C. W. Tan, M. Chiang, and R. Srikant, "Maximizing sum rate and minimizing MSE on multiuser downlink: optimality, fast algorithms and equivalence via max-min SINR," *IEEE Trans. Signal Process.*, vol. 59, no. 12, pp. 6127–6143, 2011.
- [18] C. W. Tan, S. Friedland, and S. H. Low, "Nonnegative matrix inequalities and their application to nonconvex power control optimization," *SIAM J. Matrix Anal. Appl.*, vol. 32, no. 3, pp. 1030–1055, 2011.

- [19] G. Scutari, D. P. Palomar, and S. Barbarossa, "Optimal linear precoding strategies for wideband noncooperative systems based on game theory—part I: Nash equilibria," *IEEE Trans. Signal Process.*, vol. 56, no. 3, pp. 1230–1249, Mar. 2008.
- [20] J. Wang, G. Scutari, and D. P. Palomar, "Robust MIMO cognitive radio via game theory," *IEEE Trans. Signal Process.*, vol. 59, no. 3, pp. 1183–1201, Mar. 2011.
- [21] D. Nguyen and T. Le-Ngoc, "Sum-rate maximization in the multicell MIMO multiple-access channel with interference coordination," *IEEE Trans. Wireless Commun.*, vol. 13, no. 1, pp. 36–48, Jan. 2014.
- [22] H. Al-Shatri and T. Weber, "Achieving the maximum sum rate using D.C. programming in cellular networks," *IEEE Trans. Signal Process.*, vol. 60, no. 3, pp. 1331–1341, Feb. 2012.
- [23] J.-S. Pang, G. Scutari, D. Palomar, and F. Facchinei, "Design of cognitive radio systems under temperature-interference constraints: a variational inequality approach," *IEEE Trans. Signal Process.*, vol. 58, no. 6, pp. 3251–3271, Feb. 2010.
- [24] G. Scutari, D. P. Palomar, and S. Barbarossa, "Optimal linear precoding strategies for wideband noncooperative systems based on game theory—part II: algorithms," *IEEE Trans. Signal Process.*, vol. 56, no. 3, pp. 1250–1267, Mar. 2008.
- [25] D. Niyato and E. Hossain, "Competitive pricing for spectrum sharing in cognitive radio networks: dynamic game, inefficiency of Nash equilibrium, and collusion," *IEEE J. Sel. Areas Commun.*, vol. 26, no. 1, pp. 192–202, Jan. 2008.
- [26] F. Wang, M. Krunz, and S. Cui, "Price-based spectrum management in cognitive radio networks," *IEEE J. Sel. Topics Signal Process.*, vol. 2, no. 1, pp. 74–87, Feb. 2008.
- [27] G. Scutari, F. Facchinei, J.-S. Pang, and L. Lampariello, "Equilibrium selection in power control games on the interference channel," in *Proc. 2012 IEEE INFOCOM*, pp. 675–683.
- [28] M. Anam, S. A. Basher, and S.-H. Chiang, "Mixed oligopoly under demand uncertainty," *B.E. J. Theoretical Econ.*, vol. 7, no. 1, 2007.
- [29] L. Duan, J. Huang, and B. Shou, "Investment and pricing with spectrum uncertainty: a cognitive operator's perspective," *IEEE Trans. Mobile Comput.*, vol. 10, no. 11, pp. 1590–1604, 2011.
- [30] L. Yang, H. Kim, J. Zhang, M. Chiang, and C. W. Tan, "Pricing-based decentralized spectrum access control in cognitive radio networks," *IEEE/ACM Trans. Netw.*, vol. 21, no. 2, pp. 522–535, Apr. 2013.
- [31] M. Haddad, S. E. Elayoubi, E. Altman, and Z. Altman, "A hybrid approach for radio resource management in heterogeneous cognitive networks," *IEEE J. Sel. Areas Commun.*, vol. 29, no. 4, pp. 831–842, Apr. 2011.
- [32] Y. Wu, T. Zhang, and D. H. K. Tsang, "Joint pricing and power allocation for dynamic spectrum access networks with Stackelberg game model," *IEEE Trans. Wireless Commun.*, vol. 10, no. 1, pp. 12–19, Jan. 2011.
- [33] Y. Li, X. Wang, and M. Guizani, "Resource pricing with primary service guarantees in cognitive radio networks: a Stackelberg game approach," in *Proc. 2009 IEEE Global Commun. Conf.*, pp. 1563–1567.
- [34] X. Kang, R. Zhang, and M. Motani, "Price-based resource allocation for spectrum-sharing femtocell networks: a Stackelberg game approach," *IEEE J. Sel. Areas Commun.*, vol. 30, no. 3, pp. 538–549, Apr. 2012.
- [35] M. Chiang, P. Hande, T. Lan, and C. W. Tan, "Power control in wireless cellular networks," *Foundations Trends Netw.*, vol. 2, no. 4, pp. 381–533, July 2008.
- [36] Y. Su and M. van der Schaar, "Linearly coupled communication games," *IEEE Trans. Commun.*, vol. 59, no. 9, pp. 2543–2553, Sep. 2011.
- [37] D. Fudenberg and J. Tirole, *Game Theory*. MIT Press, 1991.
- [38] F. Facchinei and J. S. Pang, *Finite-Dimensional Variational Inequalities and Complementarity Problems*. Springer-Verlag, 2003.
- [39] S. Parsaefard, A. R. Sharafat, and M. van der Schaar, "Robust additively coupled games in the presence of bounded uncertainty in communication networks," *IEEE Trans. Veh. Technol.*, vol. PP, no. 99, pp. 1–17, 2014.
- [40] E. Altman, T. Boulogne, R. E. Azouzi, T. Jiménez, and L. Wynter, "A survey on networking games in telecommunications," *Comput. Operations Research*, vol. 33, pp. 286–311, 2006.
- [41] B. Colson, P. Marcotte, and G. Savard, "Bilevel programming: a survey," *4OR*, vol. 3, no. 2, pp. 87–107, 2005.
- [42] M. Aghassi and D. Bertsimas, "Robust game theory," *Mathematical Programming*, vol. 107, no. 1, pp. 231–273, June 2006.
- [43] R. Nishimura, S. Hayashi, and M. Fukushima, "Robust Nash equilibria in N -person non-cooperative games: uniqueness and reformulation," *Pacific J. Optimization*, vol. 5, no. 2, pp. 237–259, May 2009.
- [44] J. Wang and D. P. Palomar, "Worst-case robust MIMO transmission with imperfect channel knowledge," *IEEE Trans. Signal Process.*, vol. 57, no. 8, Aug. 2009.
- [45] A. Pascual-Iserte, D. Palomar, A. Perez-Neira, and M. Lagunas, "A robust maximin approach for MIMO communications with imperfect channel state information based on convex optimization," *IEEE Trans. Signal Process.*, vol. 54, no. 1, pp. 346–360, Oct. 2006.
- [46] E. Altman, K. Avrachenkov, and A. Garnaev, "Closed form solutions for water-filling problems in optimization and game frameworks," *Springer J. Telecom. Syst.*, vol. 47, no. 1-2, pp. 153–164, 2011.
- [47] D. P. Palomar and Y. C. Eldar, *Convex Optimization in Signal Processing and Communications*. Cambridge University Press, 2010.
- [48] S. Boyd and L. Vandenberghe, *Convex Optimization*. Cambridge University Press, 2004.
- [49] T. Basar and G. J. Olsder, *Dynamic Non-Cooperative Game Theory*, 2nd ed. Academic Press, 1995.



theory in wireless networks.



Okawa Foundation Award (2006), the IBM Faculty Award (2005, 2007, 2008), the Most Cited Paper Award from the *EURASIP: Image Communications Journal* (2006), the Gamenets Conference Best Paper Award (2011), and the 2011 IEEE Circuits and Systems Society Darlington Best Paper Award. She holds 33 granted US patents, and is the founding director of the UCLA Center for Engineering Economics, Learning, and Networks.



Saedeah Parsaefard (S'09) received her B.Sc. and M.Sc. degrees from Amirkabir University of Technology (Tehran Polytechnic), Tehran, Iran, in 2003 and 2006, respectively, and her Ph.D. degree in electrical and computer engineering from Tarbiat Modares University, Tehran, Iran, in 2012. From November 2010 to October 2011, she was a visiting Ph.D. candidate at the Department of Electrical Engineering, University of California at Los Angeles (UCLA). Her current research interests are robust resource allocation and applications of robust game

Mihaela van der Schaar (SM'04–F'10) received her M.Sc. and Ph.D. degrees from Eindhoven University of Technology, Eindhoven, The Netherlands. She is the Chancellor's Professor of Electrical Engineering at the University of California, Los Angeles, an IEEE Fellow, a Distinguished Lecturer of the Communications Society for 2011–2012, and the Editor in Chief of the IEEE TRANSACTIONS ON MULTIMEDIA. She received the Best Paper Award from the IEEE TRANSACTIONS ON CIRCUITS AND SYSTEMS FOR VIDEO TECHNOLOGY (2005), the Okawa Foundation Award (2006), the IBM Faculty Award (2005, 2007, 2008), the Most Cited Paper Award from the *EURASIP: Image Communications Journal* (2006), the Gamenets Conference Best Paper Award (2011), and the 2011 IEEE Circuits and Systems Society Darlington Best Paper Award. She holds 33 granted US patents, and is the founding director of the UCLA Center for Engineering Economics, Learning, and Networks.

Ahmad R. Sharafat (S'75–M'81–SM'94) is a professor of electrical and computer engineering at Tarbiat Modares University, Tehran, Iran. He received his B.Sc. degree from Sharif University of Technology, Tehran, Iran, and his M.Sc. and his Ph.D. degrees both from Stanford University, Stanford, California, all in electrical engineering in 1975, 1976, and 1981, respectively. His research interests are advanced signal processing techniques, and communications systems and networks. He is a Senior Member of the IEEE and Sigma Xi.